

Draft

Appendix G

Solar Probe

Mission and Project Description

APPENDIX G

SOLAR PROBE MISSION AND PROJECT DESCRIPTION

TABLE OF CONTENTS

1.	INTRODUCTION	G-1
2.	OVERVIEW	G-2
2.1	SCIENCE OBJECTIVES	G-2
2.1.1	Mission Overview	G-2
2.1.2	Science Objectives	G-3
2.1.3	Measurement Requirements	G-4
2.1.3.1	<i>In Situ</i> Measurement Requirements	G-5
2.1.3.1.1	Ions and Electrons	G-7
2.1.3.1.2	Energetic Particles	G-8
2.1.3.1.3	Plasma Waves	G-9
2.1.3.1.4	Magnetic Fields	G-9
2.1.3.2	Remote Sensing Measurement Requirements	G-10
2.1.3.2.1	Imaging Solar Magnetic Fields and Small-Scale Structures	G-11
2.1.3.2.2	3-D Coronal Imager	G-15
2.1.4	Strawman Payload	G-16
2.1.4.1	<i>In Situ</i> Experiments	G-18
2.1.4.1.1	Solar Wind Ion Composition and Electron Spectrometer	G-18
2.1.4.1.2	Fast Solar Wind Ion Detector	G-19
2.1.4.1.3	Plasma Wave Sensor	G-20
2.1.4.1.4	Magnetometer	G-20
2.1.4.1.5	Energetic Particle Composition Spectrometer	G-21
2.1.4.2	Remote Sensing Experiments	G-21
2.1.4.2.1	Introduction	G-21
2.1.4.2.2	Visible Magnetograph-Helioseismograph	G-22
2.1.4.2.3	EUV Imager	G-24
2.1.4.2.4	All-Sky, 3-D Coronagraph Imager	G-24
2.2	DESCRIPTION OF SPACECRAFT CONCEPT AND MISSION	G-24
2.2.1	Reference Mission	G-25
2.2.1.1	Baseline Mission	G-25
2.2.1.2	Orbit Determination Accuracy	G-28

2.2.2	Spacecraft System Design.....	G-28
2.2.2.1	Applicable Standards.....	G-28
2.2.2.2	System Overview.....	G-29
2.2.2.3	Mass.....	G-32
2.2.2.4	Power.....	G-32
2.2.2.5	Volume.....	G-32
2.2.2.6	Thermal.....	G-33
2.2.2.7	Command, Control, and Data.....	G-35
2.2.2.8	Fields of View.....	G-37
2.2.2.9	Coordinate System and Mechanical Design.....	G-38
2.2.2.10	Attitude Control.....	G-40
2.2.2.11	Telecommunications.....	G-41
2.2.2.12	Propulsion.....	G-43
2.2.3	Launch Vehicle.....	G-43
2.2.3.1	Launch Site.....	G-43
2.2.3.2	Launch Vehicle.....	G-43
2.2.4	In-Flight And Near-Sun Environmental Hazards.....	G-43
2.2.4.1	Dust Hazards.....	G-44
2.2.4.2	Radiation Hazard.....	G-46
2.2.4.3	Outgassing-Sublimation Hazard.....	G-47
2.2.4.4	Sublimation Rates.....	G-47
2.2.4.4.1	Mass Loss Rate and Interference with Science Objectives.....	G-48
2.3	MISSION DEVELOPMENT CONCEPT	G-50
2.3.1	Flight System Design and Deliveries.....	G-50
2.4	MISSION OPERATIONS CONCEPT	G-51
2.4.1	Integrated Mission Flight Operations Team.....	G-51
2.4.2	Beacon Mode Cruise.....	G-52
2.4.3	Encounter Operations.....	G-53
2.5	PROJECT SCHEDULE.....	G-53
3.	SCIENCE INVESTIGATIONS	G-53
3.1	RESOURCES FOR THE SCIENCE INVESTIGATIONS	G-53
3.2	INTERACTION WITH THE PROJECT.....	G-56
3.2.1	Project Fiscal Policy.....	G-56
3.2.1.1	Budgetary Authority.....	G-56
3.2.1.2	Cost-Capped Mission Budget Environment.....	G-57
3.2.2	Project Organization.....	G-57
3.2.2.1	Science Investigators as Members of Project Teams.....	G-58
3.2.2.2	Relationship Between Science Teams and the Outer Planets/Solar Probe Project.....	G-58
3.2.3	Encounter Science Team Selection, Participation, and Management.....	G-59

3.2.4	Mission Assurance Requirements.....	G-59
3.2.5	Principal Investigator Responsibilities.....	G-59
3.3	DELIVERABLES.....	G-61
3.3.1	General.....	G-61
3.3.2	Hardware Delivery.....	G-61
3.3.3	Software.....	G-62
3.3.3.1	Software Documentation - Software/Computer Systems Interface Control Document (ICD).....	G-62
3.3.3.2	Software Documentation - Other.....	G-62
3.3.3.3	Software Test: Required Evaluation Procedures.....	G-62
3.3.3.4	Software Source Materials.....	G-63
3.4	PAYLOAD REVIEWS.....	G-63
3.5	DOCUMENTATION REQUIREMENTS	G-64
3.5.1	Memorandum of Agreement.....	G-64
3.5.2	Functional Requirements Document (FRD) / Experiment Implementation Plan (EIP) / Safety Plan.....	G-64
3.5.3	Ground Data System (GDS) / Mission Operations System (MOS) Requirements.....	G-65
3.5.4	Interface Control Documents (ICD's).....	G-65
3.5.5	Instrument Design Description Document (IDDD).....	G-65
3.5.6	Payload Handling Requirements.....	G-66
3.5.7	Unit History Log Book.....	G-66
3.5.8	Acceptance Data Package.....	G-66
4.	DISCUSSION OF NADIR VIEWING OPTIONS	G-66
4.1	SOLAR WIND PLASMA VIEWING OPTIONS	G-67
4.2	PLASMA VISUALIZATION MODEL	G-67
4.3	ASSESSMENT OF NADIR VIEWING OPTIONS.....	G-69
5.	REFERENCES	G-72

TABLE OF TABLES

TABLE 1.	SOLAR PROBE SCIENCE MEASUREMENT REQUIREMENTS.....	G-6
TABLE 2.	PROPERTIES OF A 4 SOLAR RADII CLOSEST APPROACH MISSION	G-13
TABLE 3.	SOLAR PROBE STRAWMAN PAYLOAD: INSTRUMENT REQUIREMENTS.....	G-17
TABLE 4.	JGA REFERENCE MISSION EVENT SUMMARY	G-27
TABLE 5.	SOLAR PROBE TELECOMMUNICATIONS PARAMETERS AT PERIHELION.....	G-42
TABLE 6.	FLUENCE OF PENETRATING 2.5-GM/CM ³ PARTICLES ON THE SPACECRAFT	G-45
TABLE 7.	SOLAR PROBE SCIENCE INSTRUMENT RESOURCE ALLOCATIONS	G-55
TABLE 8.	INVESTIGATION FUNDING PROFILE GUIDELINES	G-56
TABLE 9.	CRITERIA FOR PLASMA VIEWING OPTIONS	G-71

TABLE OF FIGURES

FIGURE 1.	THE VARIATION OF IMPORTANT PLASMA PARAMETERS FROM THE SOLAR SURFACE UP TO $20 R_S$	G-11
FIGURE 2.	VIEW OF SPACECRAFT WITH EXAMPLE PLASMA INSTRUMENT CONFIGURATION..	G-19
FIGURE 3.	INTERPLANETARY TRAJECTORY TO PERIHELION 1.....	G-26
FIGURE 4.	PERIHELION 1 TRAJECTORY AS SEEN FROM THE EARTH.....	G-28
FIGURE 5.	TYPICAL INCOMING APPROACH PERSPECTIVE.....	G-29
FIGURE 6.	SOLAR PROBE SPACECRAFT	G-30
FIGURE 7.	SOLAR PROBE FUNCTIONAL BLOCK DIAGRAM.....	G-31
FIGURE 8.	BUS TAPERED WEDGE QUADRANTS (DIMENSIONS IN MM).....	G-34
FIGURE 9.	INTEGRATED SCIENCE PAYLOAD BOOM VOLUME	G-35
FIGURE 10.	BUS INSTRUMENT FIELDS OF VIEW.....	G-37
FIGURE 11.	SOLAR PROBE SPACECRAFT COORDINATE SYSTEM.....	G-38
FIGURE 12.	TELECOMM SUBSYSTEM ARCHITECTURE.....	G-41
FIGURE 13.	SOLAR PROBE TELEMETRY RATE NEAR PERIHELION FOR QUADRATURE	G-42
FIGURE 14.	INTEGRAL SOLAR PROBE DUST PARTICLE FLUENCE.....	G-45
FIGURE 15.	OUTER PLANETS/SOLAR PROBE PRELIMINARY SCHEDULE	G-54
FIGURE 16.	ORGANIZATION CHART FOR THE OUTER PLANETS/SOLAR PROBE PROJECT.....	G-57
FIGURE 17.	SAMPLE DISTRIBUTION OF H^+	G-68
FIGURE 18.	VARIATION OF THE HALF-WIDTH OF THE OBSTRUCTION CONE	G-70

APPENDIX G

SOLAR PROBE MISSION AND PROJECT DESCRIPTION

1. Introduction

This appendix provides background information about the Solar Probe mission and pointers to the present body of relevant scientific knowledge. This information is to be used in conjunction with Appendices A and F by proposers in preparing a formal response to NASA AO 99-OSS-XX, Outer Planets Program Announcement of Opportunity.

This document contains general information, requirements, technical descriptions, and performance and interface envelopes that are pertinent to the preparation of proposals in response to the Solar Probe part of the AO. Also given is a detailed description of the activities for which the selected Principal Investigators (PI's) will be responsible. Information from the AO is repeated only if necessary for continuity of content. In the event of conflict between the provisions of the AO and any appendix, the AO takes precedence.

It is important to note that the reference mission described here is only one of several options under study. The AO which this appendix accompanies will result in the selection of a Solar Probe Remote Sensing Science Investigation and a Solar Probe *In Situ* Science Investigation, the leaders and members of which will become members of the Solar Probe Integrated Implementation Team.

The science investigations proposed by the winning teams, as well as the reference mission described in this appendix, will evolve together into an end-to-end mission that best meets the science objectives within the strict cost cap. The actual Solar Probe mission that is implemented may differ substantially from the reference mission and the details of the winning science investigation proposals.

NASA has not committed to this project, nor this reference mission, nor to any specific launch schedule, launch vehicle, power system, Project budget, or funding profile.

The word "mission" means the Solar Probe mission. "Spacecraft" includes all launched engineering hardware and software. The term "flight system" includes all launched hardware and software for both engineering and science functions. The term "Solar Probe" may be used to refer either to the spacecraft itself or to the Solar Probe mission (as in "...will be developed for Solar Probe"). The word "project" is used in this document to refer to the Outer Planets/Solar Probe Project; Solar Probe is one of the three missions assigned to this Project.

2. Overview

2.1 Science Objectives

2.1.1 Mission Overview

The solar corona is one of the last unexplored regions of the solar system and one of the most important to understand in terms of Sun-Earth Connections. SOHO, TRACE, and Ulysses results have focused understanding of regions to the point where *in situ* measurements and close-up imaging are necessary for further progress.

With the Solar Probe mission, a robust, scientifically important space mission to explore the source of the solar wind from inside the solar corona at 4 to 107 solar radii (0.5AU) from the Sun is envisioned.

The primary science objective (see also Section 2.1.2) is to understand the processes that heat the solar corona and produce the solar wind. The Solar Probe Mission will accomplish this objective with a combination of remote-sensing sensors designed to detect small-scale, transient magnetic structures at and around the Sun and *in situ* sensors designed to characterize the local heating and acceleration of plasma. The payload development will be streamlined by having each of the two classes of instruments built under the direction of a single principal investigator (or all instruments under one PI):

- ***In situ* measurements:** plasma distribution functions and composition, energetic particle fluxes and composition, magnetic fields, plasma waves;
- **Remote sensing:** Magnetograph/Doppler helioseismology, high-spatial-resolution EUV/X-ray imaging of the Sun, and coronal imaging.

The mission and spacecraft designs are partly derived from concepts developed for earlier mission studies but with important differences that result in cost savings and enhanced science return.

Solar Probe will launch in February 2007 and perform a gravity assist flyby of Jupiter in June 2008 to change the heliocentric orbit plane from the ecliptic to a solar polar orbit. The probe will make two close flybys of the Sun with the perihelion at 3 solar radii from the photosphere, one flyby at or near solar maximum in October 2010, and one in the descending phase of the solar cycle about 4.3 years later. The operations for each of the two encounters will consist of two phases: (1) Near Encounter: -1 day to +1 day from closest approach (radius of 4 to 20 R_s); and (2) Inner Heliosphere: -10 days to -1 day and +1 day to

+10 days from closest approach (107 to 20 R_s). In addition there will be instrument checkout and calibration and cross calibration with existing, near-Earth instruments when Solar Probe is close to 1 AU.

2.1.2 Science Objectives

The Solar Probe mission is intended to achieve a set of specific scientific objectives. The primary science objectives, called the "Group 1 objectives," represent the irreducible baseline objectives of the mission. The secondary science objectives, called "Group 2 objectives," are of high scientific importance, but not so critical for this mission as to fall within the irreducible baseline. The tertiary objectives, called "Group 3 objectives," are objectives that could be addressed only with additions to the core payload.

Group 1 Objectives

- Determine the acceleration processes and find the source regions of the fast and slow solar wind at maximum and minimum solar activity;
- Locate the source and trace the flow of energy that heats the corona;
- Construct the three-dimensional density configuration from pole to pole, and determine the subsurface flow pattern, the structure of the polar magnetic field and its relationship with the overlying corona; and
- Identify the acceleration mechanisms and locate the source regions of energetic particles, and determine the role of plasma turbulence in the production of solar wind and energetic particles.

Group 2 Objectives:

- Investigate dust rings and particulates in the near-Sun environment;
- Determine the outflow of atoms from the Sun and their relationship to the solar wind; and
- Establish the relationship between remote sensing, near-Earth observations at 1 AU and plasma structures near the Sun.

Group 3 Objectives:

- Determine the role of x-ray microflares in the dynamics of the corona; and
- Probe nuclear processes near the solar surface from measurements of solar gamma rays and slow neutrons.

2.1.3 Measurement Requirements

Selected investigations must be prepared to meet the Group 1 objectives of the Solar Probe mission during the Near Encounter and Inner Heliosphere operations periods of the mission as well as the minimum required checkout, calibration and cross-calibration requirements.

In order to achieve the aims of the Solar Probe Mission, it will be necessary to perform suitable *in situ* measurements of the high- and low-speed solar winds and coronal plasma and remote-sensing measurements of the coronal base, the upper chromosphere, and the supergranular network from heliocentric radii of $\sim 4\text{--}20 R_{\odot}$. The acceleration of the solar wind and the heating of the corona are likely linked in a very intimate fashion. By looking for remote features that can link with *in situ* measurements, e.g., the heat flux in the various ion distributions, the connection between photospheric dynamics and coronal energetics can be established. Determining the acceleration processes and source regions for the fast and slow solar wind at solar minimum and solar maximum requires both a full suite of plasma state measurements (distribution functions, composition, magnetic field and wave environment), as well as remote sensing to set the context of the measurements.

These requirements can be met, if the trajectory of the spacecraft over the Sun is polar and the encounter takes place during a period in which well-developed polar coronal holes are present. Such a trajectory will permit high-speed solar wind measurements to be made over the poles of the Sun. It will also permit measurements to be made within closed coronal structures, coronal streamers, and the low-speed solar wind near the equator. Remote sensing measurements with high spatial resolution will be possible both in the polar (open) and low-latitude (closed) magnetic field regions. Allowance should be made for the possibility that the magnetic field and streamer structure is not as simple and symmetrical as some models suggest.

Slow and fast solar wind regions will be sampled by the polar trajectory of solar probe, while sampling near both minimum and maximum solar activity periods is achieved by two perihelion passes separated by ~ 5 years. Actually matching up *in situ* measurements with distinct surface features is problematic; however, the magnetic field beneath the trajectory, as well as the temperature and density structure, are required for setting the context of the wind through which the probe is flying.

The minimum measurement requirements for success are:

- Characterize the solar wind within a high-speed stream
- Characterize the plasma in a closed coronal structure, viz., a coronal streamer, and probe the subsonic solar wind
- Image the longitudinal structure of the white-light corona from the poles
- Produce a high-resolution image in each available wavelength band, preferably in a high-latitude region
- Characterize the plasma waves, turbulence and/or shocks, etc., that are causing coronal heating
- Determine the differences in solar wind characteristics during solar minimum and solar maximum

Table 1 quantifies measurements that fully meet the Group 1 objectives. If a proposer believes the Group 1 objectives can be met with other or less stringent measurements, this should be addressed in the body of the proposal. The rationale for these measurement requirements is detailed in the following sections.

2.1.3.1 *In Situ* Measurement Requirements

Almost all current information about energetic particles from the Sun comes from measurements at 1 AU, with the exception of data from the Helios spacecraft that was as close as 0.3 AU. The solar particles interact with the interplanetary medium through which they have traveled, and as a result, the measurements are not a true reflection of the particle distributions and composition close to their origin. The basic unanswered questions of how they are accelerated and fractionated can only be answered by *in situ* measurements on a Solar Probe Mission.

The goal of the *in situ* science package is to measure those unknown details of the particles and fields in the corona that will reveal how the corona is heated and the solar wind accelerated. In order to focus on this goal, the measurement requirements must be optimally designed to cope with the anticipated bulk properties of the solar wind and possible closed structures at radii as close as $4 R_{\odot}$ from the Sun's center.

Observations over the past six years, in particular with *Ulysses*, have shown that the composition of the solar wind plasma gives the most direct information about the source region of the solar wind and its characteristics. Recent measurements of highly unusual compositions in the Coronal Mass Ejection's (CME's) observed in the slow in-ecliptic wind at 1 AU give clues to the complex mix of plasmas originating in both hot and cold regions of the corona and their evolution during transit from their source to 1 AU. Studies of the

Table 1. Solar Probe science measurement requirements, 0.5 AU to 4 R_S to 0.5 AU. Two passes: The first near solar maximum and the second near solar minimum

Parameters or Quantity Measured	Sensitivity (Dynamic Range)	Spectral Range (Resolution)	Viewing	Resolution, Time Spatial Resolution at Perihelion (over poles)
Vector magnetic fields	0.05 nT (5 nT to 10 ⁴ nT)			10 ms (10 ms) 3 km (1.5 km)
Time averaged distribution functions of H ⁺ , ³ H ⁺⁺ , ⁴ He ⁺⁺ , C ^{+X} , O ^{+X} , Si ^{+X} or Fe ^{+X}	10 km s ⁻¹ (2 x 10 ⁷)	0.05-10 keV/e	Nadir 10° x 10° and 135° x 300° (2.5 sr)	1s (300 km) for H, He, e ⁻ 10s for heavy ions
Spectra of energetic particles by species: H ⁺ , ³ He ⁺⁺ , ⁴ He ⁺⁺ , C ^{+X} , O ^{+X} , Si ^{+X} , or Fe ^{+X} , e ⁻	10 cm ⁻² s ⁻¹ sr ⁻¹ keV ⁻¹ (10 ⁷)	0.02<E<20 MeV/n e ⁻ : 0.02 -1.0 MeV (E/E) < 0.07	135° x 300° 20° x 20°	5s protons 30s others
Vector Electric and Vector Magnetic Oscillations	Threshold: 10 ⁻⁵ Vm ⁻¹ 10 ⁻⁹ (nT) ² /Hz (10 ⁶)	10 Hz to 150 kHz	4 sr	1 ms: 1 μs snapshot, 1s spectral
Fast distribution functions of H ⁺		0.02 - to 5 keV (E/E = 0.07)	90° x 300°	1 ms (4 ms)
High spatial resolution of atmosphere temperatures at different heights	10 ² erg cm ⁻² sr ⁻¹	8Å at EUV wavelengths	Solar disc	5 arc sec < 1s exposure
Magnetic field (line of sight) velocity field	10 G (10 to 3000 G) 20 ms ⁻¹ (10 - 4000 ms ⁻¹)	8Å (if visible) 70mÅ	Solar disc	2 arc-sec (32 km) 2s
Solar corona (white light)	Signal to noise >100	400 to 700 nm	20° - 180° from s/c - Sun line (<1°)	<1min

evolution of the solar wind over distances of several AU reveal that the mapping back to the source region becomes increasingly more uncertain with increasing distance. Even the best measurements of the terminal solar wind at 1 AU will not give us the definitive answer on how the solar wind is formed.

It is, thus, clear that, in order to understand solar wind acceleration and pinpoint the wind's source region, it is imperative to characterize the solar wind in, or as close as possible to, the regions where its acceleration takes place. To achieve this it will be essential to find, for example, the dependence on altitude of fundamental kinetic parameters (bulk speed, temperature) and on non-Maxwellian features for a number of ion species as well as for electrons. The determination of the velocity distributions of a number of key ions as well as electrons is, therefore, an essential component of the Solar Probe measurement requirements to meet the first two Group 1 objectives.

2.1.3.1.1 Ions and Electrons

The ion measurements are of special significance to the mission and accordingly take a substantial fraction of the resources devoted to the *in situ* measurements. In addition to protons and electrons, the distribution functions (from which key kinetic parameters can be derived) of dominant charge states of, e.g., He, C, O, Ne, Si and Fe should be measured with a time resolution of ~10 sec. Charge state spectra for these elements should also be obtained. The energy range should be as wide as possible. Near perihelion the probe thermal shield obscures the trajectories of particles coming from the direction of the Sun. This "shadow" cuts into the bulk of possible measurements of the distribution function of ions. The effect is mitigated somewhat by the aberration of solar-wind flow, depending, in turn, on the wind bulk flow speed. However, aberration does not fully solve the problem, and nadir viewing and a wide field of view are essential for measurements of the complete velocity distributions, which are expected to be broad and complex in the solar wind acceleration region. In order to make satisfactory measurements of the angular distribution of the ions in particular, nadir viewing may be required, with a set of ports looking towards the Sun. (See Section 4 of this volume for a discussion of why observing the fast solar wind requires nadir viewing.)

All species, including electrons, can be expected to have anisotropic distribution functions, with suprathermal components that may reflect the nature of the heating process and that may be important for heat transfer. These features, as well as the detailed knowledge of the electromagnetic and electrostatic waves present, can provide very clear indications of the nature of the heating process well outside the main heating region.

If plasma microphysics plays an expected fundamental role in the physics of the corona, then to adequately address the first, second, and fourth Group 1 objectives, very fast, but more

limited, ion measurements are required in addition to those provided by plasma and particle spectrometers. One of the main theoretical ideas for coronal heating is the damping of the cyclotron/Alfvén waves in the solar corona. Such processes can occur on the time scale of the cyclotron period, which will be ~ 400 Hz at $4 R_{\odot}$. Extreme ion distribution functions have been inferred from SOHO ultraviolet spectrometer observations. If these inferences are correct, relaxation of this "free energy" in the form of wave generation and resonant wave-particle interactions will occur. Again, temporal scales are expected to be as fast as the proton/ion gyroperiods. Thus, to understand fully the physical processes of coronal ion heating and thermalization, measurements of the distribution functions are required on gyrofrequency time scales.

2.1.3.1.2 Energetic Particles

Solar energetic particle events have been subdivided into two main classes. Impulsive events are enriched in heavy ions, most prominently in Fe and most of the time also in ^3He , while gradual events resemble more closely the photospheric composition, with some mass and ionization-potential-related bias (e.g. Reames 1992). The acceleration in impulsive events is thought to occur in the flare site with resonant wave absorption being responsible for the drastic ^3He enrichment, whereas the gradual events are believed to be associated with CME-driven shocks that are effective up to much larger distances from the Sun. Close to the Sun, angular and energy distributions will be largely free of interactions with the interplanetary medium, so measurements of the composition and angular and energy distributions of the particles from both types of events at Solar Probe will, along with magnetic field data, provide the information necessary to determine the origin and mechanism of acceleration and fractionation.

The large particle fluxes close to the Sun will result in a substantial increase in sensitivity, in particular to small impulsive events. The increase in sensitivity is counterbalanced by the short time of data acquisition and the fact that large energetic particle events do not occur continuously. However, there is ample evidence that small solar flares, or "microflares," occur at a high rate (e.g. Lin et al., 1992; Biesecker et al., 1993). It can be expected that these events produce energetic particle fluxes below the sensitivity level of instruments at 1 AU, but they should be detectable closer to the Sun. Also, impulsive events occur on average at a rate of 2 - 3 per day on the solar disc during solar maximum (Reames et al., 1994). Since Solar Probe will pass perihelion twice, that is, once each during both solar maximum and solar minimum, it can be expected that several impulsive events and a good sample of microflares will be observed during the ~ 5 days when Solar Probe will be within distances smaller than 0.3 AU. The closer to the Sun the events are observed, the more useful they will be to separate interplanetary effects from local acceleration.

The energetic particles measurement should be designed to detect the possible presence of suprathermal particles, which might play a role in accelerating the solar wind, and also to detect any trapped particle population in magnetically closed regions. It should be sufficient to determine the distribution function of electrons, protons, and perhaps one or two other species to satisfy the Group 1 objectives.

2.1.3.1.3 Plasma Waves

The second and fourth Group 1 objectives require the characterization of magnetohydrodynamic (MHD) and plasma turbulence that may induce plasma heating. Scintillation measurements made through the corona using both natural sources and spacecraft transponders have shown that turbulence in the corona is ubiquitous. However, the dynamical and energetic role of the turbulence in accelerating and heating the solar wind remain unknown. Electromagnetic waves are the most likely source of this turbulence. Previous space missions employed magnetometers sampling the quasistatic magnetic field to detect MHD waves, but the high field magnitudes and rest frame velocities predicted for the Solar Probe mission mandate that these measurements must be carried out by a plasma wave system with the proper frequency coverage (see Figure 1). Compared with waves observed in the Earth's magnetosphere and the local solar wind, the wave amplitudes in the solar corona could be extremely large (for energies $<10\%$ of the solar wind energy flux, the peak rms field strengths should be of order 0.001–0.01 G over frequencies up to several hundred Hz). Thus, the sensor instrumentation (preamplifiers, searchcoils, electric field antenna, etc.) need not be as sensitive as previously flown, if these models are correct. On the other hand, nonlinear waves have been suggested as a source of heating (Temerin et al. 1986). Detection of such waves requires very high time resolution measurements. Other emissions of interest in this regime will be whistler waves that may be involved in electron thermalization and will occur at higher frequencies. Electrostatic emissions associated with particle beams and shock-like structures are expected.

2.1.3.1.4 Magnetic Fields

Precise and accurate measurements of the orientation and intensity of the coronal magnetic field are essential to the achievement of all Group 1 objectives. Knowledge of the large-scale coronal magnetic structure is fundamental to the modeling and analysis of solar wind flow and energetic particle transport. On shorter scale lengths, the magnetic field is diagnostic of the rate of magnetic dissipation in regions where reconnection is taking place, the structure of current sheets and other types of discontinuities, the properties of helical magnetic structures such as flux ropes, and the propagation characteristics and strength of shock fronts. Finally, low frequency (< 1 Hz) MHD waves must be accurately detected and analyzed in order to assess their role in solar wind heating and acceleration.

The large-scale solar magnetic field at $4 R_S$ is expected to be on the order of 0.1 G. However, due to the very dynamic nature of the corona, it would be prudent for a vector magnetometer to be able to measure magnetic fields as great ~ 0.6 G, in order to provide margin and accommodate the unexpected. The magnetometer must be sensitive to perturbations as small as 10^{-6} G in order to fully characterize the power spectrum of waves and fluctuations out to a radial distance of $\sim 30 R_S$. Finally, the high speed of the spacecraft at perihelion, ~ 300 km/s, and the need to analyze thin structures implies a minimum sample rate of at least 10 vectors per sec (i.e., ~ 1 measurement per 30 km) and makes the option for "burst" sample rates of ~ 100 vectors per second highly desirable.

The near-equatorial magnetic fields may be closed, as well as sloughed-off "plasmoids" that SOHO coronal measurements have recently discovered. Large amplitude, low frequency Alfvén waves are expected, and these fields superposed on top of the ambient may significantly alter the viewing of plasma detectors placed on Solar Probe as discussed in Section 4.

2.1.3.2 Remote Sensing Measurement Requirements

High-resolution observations in the visible, EUV, and X-Ray regions of the spectrum allow measurements of the fine structure of the magnetic field and the density structure of the corona that are fundamental to plasma and particle acceleration. Lower resolution observations provide data on the state of the corona during the encounter and provide context for the particle and fields measurements. Low-resolution observations with large fields of view also allow tomographic reconstruction's of the three-dimensional structure of the corona.

The Solar Probe Mission provides a unique platform for very high-resolution imaging of the solar surface and the extended corona. There are three principal advantages of a near-Sun platform for imaging experiments:

1. **Measurements of the polar regions**, which are inaccessible from ecliptic plane-based observations;
2. **High spatial resolution in the visible, X-Ray, and EUV** because of the very close proximity to the Sun;
3. **Three-dimensional coronal mapping by tomography** because of the rapid change in perspective provided by the spacecraft orbit.

Visible, EUV, and/or X-ray imaging can be used to measure the polar magnetic field, establish the size and cospatiality of magnetic structures in the photosphere and the location of high temperature gas, and to determine the 3-dimensional structure of the white light corona.

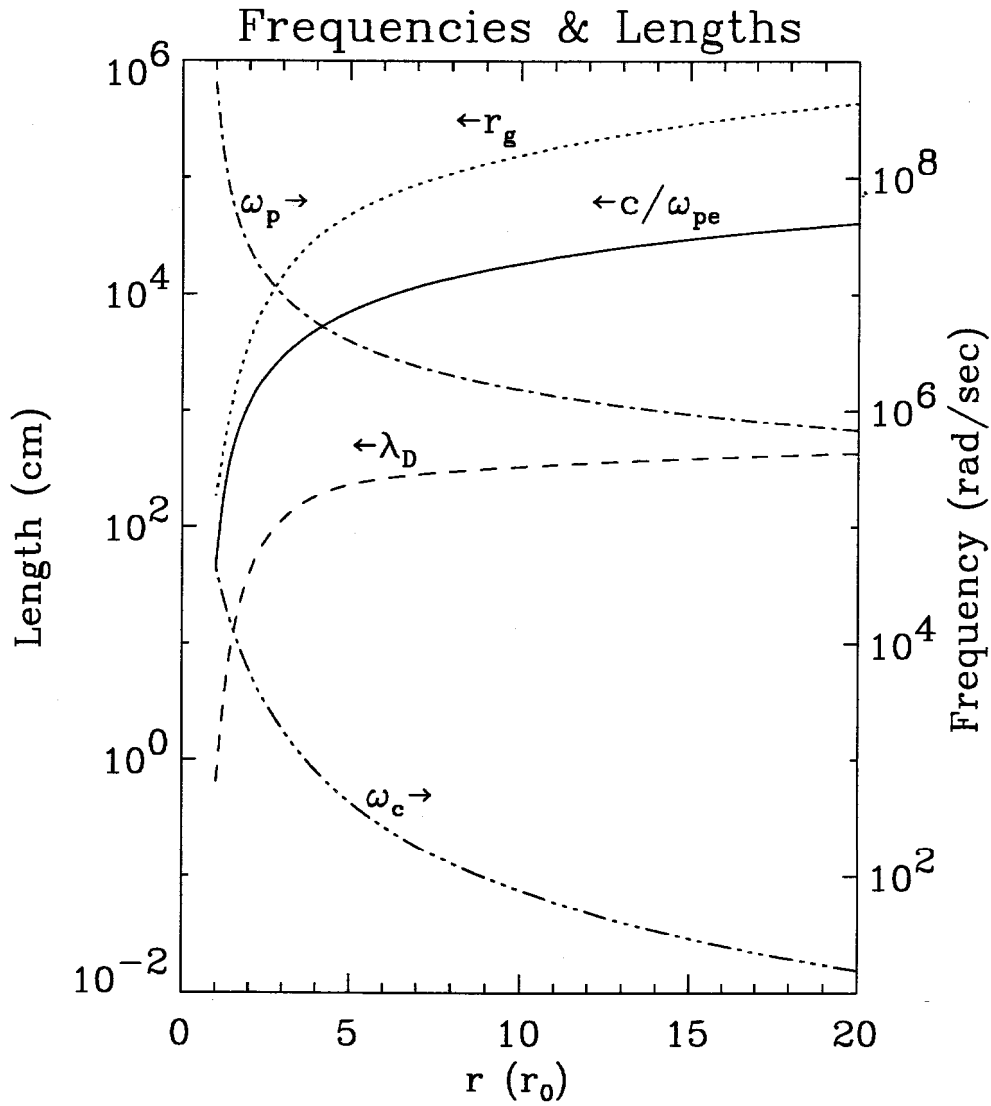


Figure 1. The variation of important plasma parameters from the solar surface up to $20 R_s$ according to the model of the Solar Probe Science Definition Team

2.1.3.2.1 Imaging Solar Magnetic Fields and Small-Scale Structures

The polar regions of the Sun can only be explored at very oblique angles from the Earth. As a result, we know far less of about the magnetic and atmospheric structures near the poles than near the equatorial regions. By using interferometer measurements, it is possible to obtain enough spectroscopic data to accurately measure the magnetic flux in regions along the path of a polar-orbiting spacecraft.

High-resolution observations in the visible, EUV, and X-Ray regions of the spectrum allow measurements of the fine structure of the magnetic field and the density structure of the corona that are fundamental to plasma and particle acceleration. Determination of the size and temporal evolution of magnetic flux elements as a function of solar latitude and type of Sun (quiet, active, plage, and coronal hole) is a primary goal. It is necessary to observe the topology of the fields and the surrounding flows and to determine the size and interaction rates of magnetic reconnection processes (which Yohkoh observations suggest are ubiquitous in the closed field corona). Spatial resolution of about 20 km at the solar surface is required to adequately characterize the phenomena of interest.

Indirect evidence supports the existence of small structures in the solar atmosphere. Radio scintillation observations of the corona have been used to argue for density fluctuations on the scale of 1 km. Comparison of the plasma density with the emission volume for density-sensitive lines in the transition region and corona yields filling factors of 10^3 to 10^5 . This may indicate structuring on the scales of 300 km down to 30 km. The smallest scales directly observed in the solar surface are magnetically related bright points seen in continuum radiation. These structures have measured sizes as small as 130 km. Deconvolution of the telescope transfer and atmosphere blurring indicates an intrinsic size on the order of 100 km. The size distribution of these bright points peaks at the limiting spatial resolution of the best solar telescopes on Earth, which indicates that there may be even smaller structures present on the visible surface of the Sun. The cool corona seen in the H α line also exhibits structures at the diffraction limit of the best Earth-based telescopes - 150 km. Images in soft X-rays show long loops that are resolution-limited with 2.5 arc-s pixels - 1800 km. Similar loops seen in EUV images are resolution limited with 1 arc-s pixels - 1000 km.

In order to understand the optical design that would drive disk imaging, it is essential to understand the conditions imposed by a near-parabolic orbit with closest approach at the solar equator. Table 2 contains properties for the 4 R_S closest approach case. The Table has been constructed with a strawman telescope so that the resolution at 75° latitude approach is 75 km. This choice has been made because the mean free path for photons in the midphotosphere is between 50 and 100 km in the visible. Because Solar Probe approaches closer to the Sun as it nears the equator, this choice will allow scientists to investigate the continuum and optically thin structures with even higher resolution over most of the surface. A telescope with an angular resolution of 2.27 arc-s is assumed for this table.

As a strawman disk-imaging design goal, an imaging resolution of about 20 km at 4 R_S is recommended. This is more than an order of magnitude better in aerial resolution than would be provided by the largest future orbiting solar telescopes that have been seriously studied

(from 1 AU, 75 km is the highest spatial frequency passed by a 1-meter telescope at 5000Å.)

Table 2. Properties of a 4 solar radii closest approach mission

The rows of Table 2 show the distance from the center of the Sun to the spacecraft in R_S , the spatial resolution of the strawman telescope in km, the velocity of the spacecraft in km/s, the time to cross the equator in hrs, the velocity toward the Sun in km/s, the velocity of the point on the surface on the line connecting the center of the Sun and the spacecraft, the rotation rate of the spacecraft in $^\circ/\text{hr}$ assuming that Solar Probe is always pointed along the Sun center line, the time to move a pixel (one half a resolution element), the number of pixels in the 15° latitude interval, the wavelength shift in Å, and the interferometer tilt angle required to compensate for the wavelength shift.

Property true anomaly latitude	=75 +75	=90 +90	=105 +75	=120 + 60	=135 + 45	=150 +30	=165 +15	=180 +0
Distance (Solar Radii)	10.8	8.0	6.36	5.33	4.69	4.29	4.07	4
Spatial Resolution (km)	75.0	53.6	41.0	33.2	28.2	25.2	23.0	23.5
Velocity (km/s)	188.	218.	245.	267.	285.	298.	306.	309.
Mission Time (Hours)	10.2	6.68	4.6	3.2	2.2	1.37	0.663	0
Velocity To Sun (km/s)	149	154	149	134	109	77.2	40.0	0
Velocity Surface (km/s)	10.6	19.3	30.6	43.4	56.2	67.2	74.6	77.2
Rotation Rate ($^\circ/\text{hr}$)	3.14	5.72	9.06	12.9	16.7	19.9	22.1	22.9
Time to Move Pixel (sec)	3.54	1.39	.671	.382	.251	.187	.158	.149
Number of Pixels	5,811	7,835	9,940	11,967	13,731	15,042	15,742	-
WL Shift (Å@6302Å)	3.13	3.24	3.13	2.81	2.29	1.62	.839	0
Tilt Angle (deg@6302Å)	2.71	2.76	2.71	2.57	2.32	1.95	1.4	0

Expansion velocities of granules in the photosphere have been observed to be 5 km/sec. Recent numerical simulations of the top of the convection zone contain shocks. Since the surface sound speed is 10 km/s and the desired resolution at $4 R_S$ is 20 km, the time between exposures should be a few seconds. Because of limited telemetry rate, it will not be possible to simply transmit long time-sequences of images, and much of the scientific data will depend on onboard image processing. Existing feature recognition software can be used to identify the magnetic bright points and then create distribution functions of their diameter, contrast, displacement velocities, and rate of change in intensity. Blocks of characteristic images should be transmitted approximately every 10 degrees of solar latitude. The statistical properties of the magnetic elements observed can be used to determine the temporal cadence of the images transmitted.

In the EUV, the regions emitting light are optically thin, so, in principal, arbitrarily fine structures can be observed. The most desirable measurements are the topology, density, temperature, and velocity of the coronal structures. In the EUV, only fleeting rocket flights have captured images of 1 arc-s quality. The flight of the Transition Region and Coronal Explorer (TRACE), which was launched in April 1998, is expected to continue to produce time sequences with 1 arc-s resolution. These data will disclose the fine-scale temperature structure of the chromosphere, transition region, and low-temperature corona. Solar Probe then should have as a priority very high resolution observations of the transition region and coronal structures.

Two representative spectral lines, peaking at 10^5 K and 10^6 K respectively, such as He 304 Å and Fe_X 171 Å, will provide information regarding the origin of structures and their spatial distribution within the boundaries of supergranular cells. Emission at coronal temperatures of 10^6 K yields the connection between their origin and their extension into interplanetary space.

The requirements for EUV imaging are determined by measurements at $4 R_S$, where the field of view is the smallest for a fixed angular aperture. A field of view of 10^5 km, or the equivalent of a few supergranular cells at $4 R_S$, defines a required angular field of view of 2.7° . The corresponding spatial resolution at that distance might be about 400 km. Such a field of view should be imaged in the 304 Å and 171 Å lines. In addition, a smaller field of view corresponding to about 5000 km at $4 R_S$ should be imaged in 304 Å to achieve a spatial resolution of ~30 km. A total of 15 images in each spectral line should be acquired, at a rate of approximately one per 10° .

In the soft X-ray, a spatial resolution of ~45 km from $4 R_S$ is required. A reasonable image field of view of $\sim 0.5^\circ$ covering 2.5×10^4 km should be possible.

2.1.3.2.2 3-D Coronal Imager

Most of the corona is optically thin, so that an imager will see the sum of all structures in the line of sight. Tomographic techniques can be applied to isolate individual coronal structures. As an example, X-ray tomography has been attempted using time sequences of Yohkoh data. This has yielded some interesting results, but because the Sun rotates at about $13^\circ/\text{day}$, the image reconstruction is confused by the evolution of coronal structures. Near closest approach, a $4 R_S$ probe rotates its perspective of the Sun nearly a factor of 40 faster than solar rotation. This is sufficient to effectively freeze a significant fraction of coronal features for tomographic studies.

The Solar Probe spacecraft and *in situ* instrumentation sample only a small volume of the coronal plasmas. To correlate these measurements with actual structures in the solar corona, a 3-D image of the corona is required. The white-light corona is generated from Thomson scattering of photospheric radiation from ambient free-coronal electrons. The image of the white-light corona reflects the integral of the electron density along the line of sight after appropriately accounting for geometrical factors and the variation of the ambient solar radiation along the line of sight. A modest 3-cm coronagraph placed on the spacecraft has a spatial resolution in the plane of the sky equivalent to an Earth-based coronagraph of ~ 1.5 m diameter. The primary measurement objectives are: 1) obtain sufficient white-light observations during the solar encounter to create a 3-D map of the global structures of the solar corona, 2) probe the corona for filamentary structures with unprecedented resolution, and 3) obtain the first direct view of the longitudinal structure of the solar corona from the poles.

The solar corona has a great deal of structure, and knowledge of this structure provides information on the connection between the photosphere and the heliosphere. Plasma near the Sun is highly ionized and is, thus, in the low-beta, near-solar regions; it is tightly bound to the coronal magnetic fields.

As Solar Probe moves from the solar pole to the equator and then to the other pole, it will first fly through the thin ($2\text{--}3^\circ$), long lasting (> 2 days) extended (to $> 30 R_S$) polar plumes. An all-sky camera will be used to make images of these structures at predetermined intervals along the spacecraft trajectory and, by differencing techniques and tomography (assuming time stationarity), will provide Solar Probe the context of what the spacecraft has flown into/out of. At the present time, it is uncertain whether the high-speed solar wind is accelerated within plumes or within intraplume regions or both. With simultaneous high-spatial-resolution field and particle measurements, this should be determined.

Solar Probe will next fly into the helmet streamer (near equatorial) region. Here, the plasma densities are considerably higher, and, thus, the images will be dominated by these low-latitude structures. Recent SOHO observations indicate that the solar wind may start acceleration at 2-3 R_S , rather than at the base, thus implying closed magnetic fields may dominate up to these distances. It is, therefore, possible that closed field regions can exist to 4 R_S and beyond. The coronal imaging and simultaneous field and particle measurements will examine these possibilities.

2.1.4 Strawman Payload

The strawman payload is based on the Group 1 objectives as defined herein by the Science Definition Team, with implementation in terms of instruments based upon the winning proposals submitted to the NRA for Solar Probe Instrument Development (NRA 95-15, 1995). However, the strawman payload is not identical to the NRA selection. For example, although X-ray and/or EUV instruments are desirable for imaging the corona, and both instruments were selected for further study under the NRA, in view of the limited payload and overlapping objectives of these instruments it would seem reasonable to fly one or the other, but not both. The sample payload discussed herein assumes that the EUV imager would be flown, but the decision as to which type of instrument is actually to be flown will be undertaken during the payload selection process based upon the proposals received in response to this AO.

The strawman payload described here is one conceptual design that allows Solar Probe to meet all of the Group 1 objectives. As such it represents one possible implementation solution based upon near state-of-the-art engineering capabilities at the concept-design level. The mass, power, and data-rate characteristics do not represent a unique solution but do show the type of tradeoffs required in assembling a complete payload on such a resource-constrained mission. Technology advances, especially in the field of miniaturization of electronics, suggest that a reduction in payload mass of more than a factor of ~6 from designs of a decade ago should be attainable for addressing the science questions that remain essentially unchanged.

It is essential, if the mission is to be both low-cost and well-focused, that the plasma science objectives and the remote sensing objectives each be addressed by integrated experimental packages (or package) in which an appropriate balance of resources is maintained. The individual components of the plasma science and remote sensing experiment package(s) should be designed to perform no more than the task required of them, and resources should be concentrated on the most critical measurements.

The following strawman list is an illustrative science payload that, if properly realized, would satisfy the primary objectives of the Solar Probe mission. It is comprised of two integrated

instrument packages consisting of five *in situ* and three remote-sensing miniaturized instruments:

- The ***In Situ Science*** package consisting of a
 - Solar Wind Ion Composition and Electron Spectrometer
 - Fast Solar Wind Ion Detector
 - Plasma Wave Sensor
 - Magnetometer
 - Energetic Particle Composition Spectrometer
- The **Remote Sensing Science** package consisting of a
 - Visible Magnetograph-Helioseismograph
 - EUV Imager
 - All-sky 3-D Coronagraph Imager

Table 3 gives the estimated resource requirements for this strawman payload from the results of an earlier study (NRA 95-15, 1995). The allocation for the Solar Wind Ion Composition and Electron Spectrometer includes some allowance for a nadir-viewing deflector.

Table 3. Solar Probe strawman payload: Instrument requirements

Strawman Instruments	Mass (kg)	Power (W)	Data Rate (kbps)
Remote Sensing Instrument Package			
Visible Magnetograph-Helioseismograph	3.0	1.2	30
EUV Imager	3.0	1.2	30
All-sky, 3 - D Coronagraph Imager	2.8	2.0	2
<i>In Situ</i> Instrument Package			
Magnetometer (with boom cables)	0.8	0.5	1.2
Solar Wind Ion Composition and Electron Spectrometer (including nadir-viewing shield system)	4.4	4.4	15.6
Energetic Particle Composition Spectrometer	0.7	0.6	4.8
Plasma Wave Sensor (with boom cables)	2.5	2.5	9.6
Fast Solar Wind Ion Detector	1.0	1.5	19.2

In this strawman, sampling techniques are mentioned only to indicate that at least one possible science implementation solution exists. The architecture of the integrated packages is not described. What is provided is a guide to how the investigations could respond to the science objectives through the use of instruments with particular choices of spectral range and resolution, sensitivity and dynamic range, field of view range and angular resolutions, and time and spatial resolution. The final selection, depending on instruments proposed to the AO, may in fact be substantially different.

2.1.4.1 *In Situ* Experiments

2.1.4.1.1 Solar Wind Ion Composition and Electron Spectrometer

The strawman plasma instrument provides a study of thermal ions and electrons within the upper corona of the Sun and near solar wind. Electrostatic mirrors and a miniature heat shield are used to direct ions and electrons within the nadir field-of-view (i.e., solar direction) into the field-of-view of a spectrometer with a steering lens and common collimator for the ion and electron sections of the spectrometer. The spectrometer is located within the umbra of the spacecraft and will be at room temperature. With this design, the effect of scattered UV light into the spectrometer is minimized. The field-of-view of the electrostatic mirror system is approximately centered on the Sun with a conical half angle of 30°. A second spectrometer of similar design is deployed below the bus of the spacecraft to provide viewing in the oblique direction. Here the spectrometer has a 290° field-of-view in the orbit plane of the spacecraft and employs a steering lens to give a 40° field-of-view orthogonal to the orbit plane. Combined, the plasma instrument provides a nearly 3-D coverage of the solar wind ions and electrons. The mounting of the plasma instrument with the spacecraft is shown in Figure 2, while the field-of-view coverage is shown in Figure 10. For ions and electrons, the nadir viewing spectrometer provides 5° x 5° angular resolution, while the oblique spectrometer provides 5° x 22.5° angular resolution.

The plasma instrument provides 2-D measurements of the ions and electrons every 2 seconds, while 3-D measurements are provided every 12 seconds. The 2-second resolution will allow resolution of structures > 600 km wide. The maximum estimated data rate is 14 kbps, which can be supported far from the Sun, while near the Sun every fifth spectrum can be transmitted and the remaining stored onboard and transmitted later when the telemetry rate is high again.

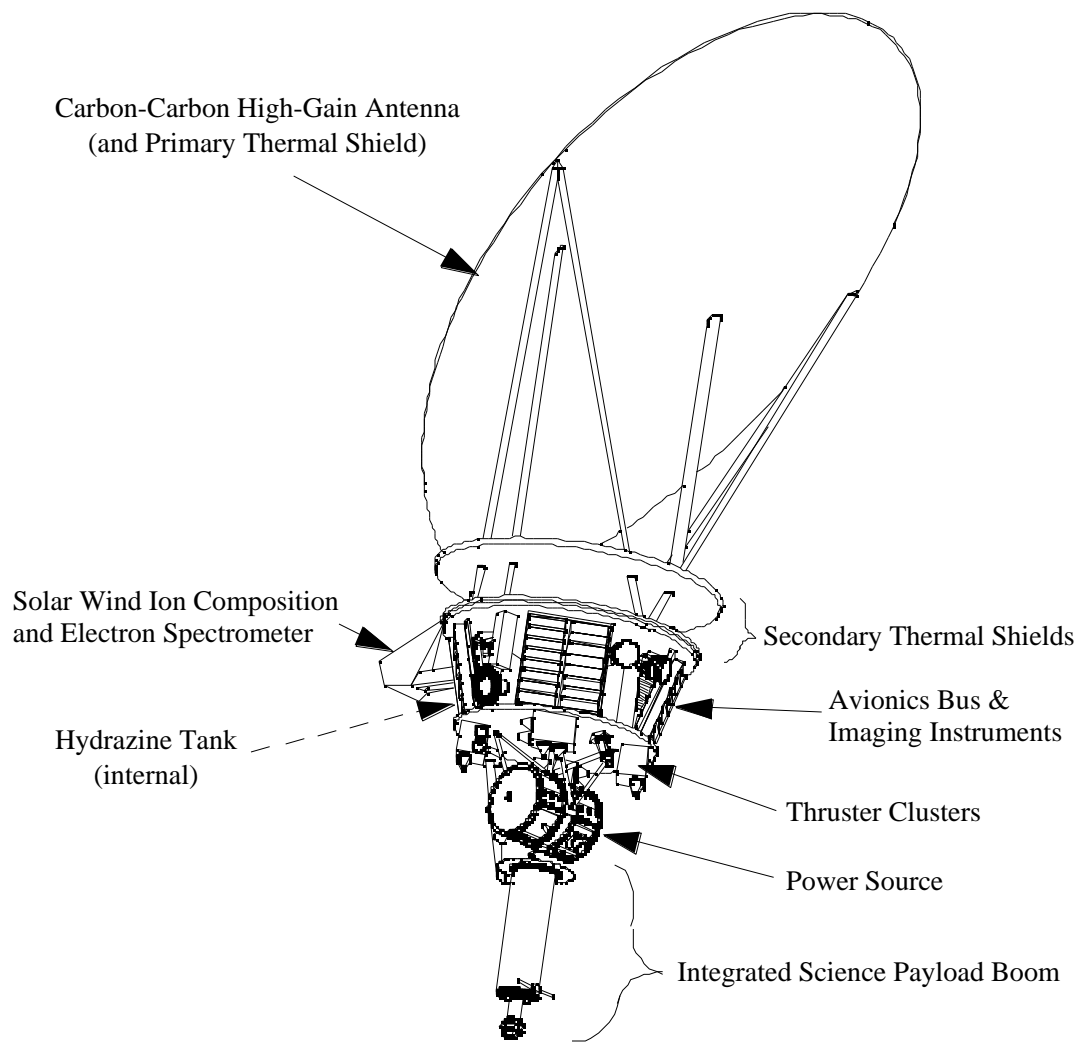


Figure 2. View of spacecraft with an example plasma instrument configuration. The electrostatic mirrors which direct the solar wind ions and electrons within the nadir field-of-view into the spectrometer field-of-view are shown. The first mirror is housed within the roof shaped miniature heat shield extending out from the end of a boom.

2.1.4.1.2 Fast Solar Wind Ion Detector

A Fast Solar Wind Ion Detector resolves ion characteristics on the scale of an ion gyroperiod in cadence with the Plasma Wave Sensors to examine the role of wave-particle effects in the acceleration (and heating) of the wind. The plasma analyzer employs new, light-weight

detectors, capable of making 3-D distribution function measurements on time scales of 10^{-2} s. These sensors use delta-doping of solid-state surfaces to reduce the dead-layer of the material, allowing for direct energy determination of incident low-energy solar wind particles. This eliminates the need for energy scanning using large electrodes or magnets and allows for great simplification of particle detection. The high fluxes near the Sun are particularly suitable for the small surface area of sensors of this type. The field of view of this instrument does not include the nadir direction. It would be mounted on the aft boom structure shown in Figure 2 yielding a 4π -sr view minus the umbral cone (see Section 2.2.2.8).

2.1.4.1.3 Plasma Wave Sensor

The high field magnitudes and rest-frame velocities predicted for Solar Probe mandate that magneto-hydrodynamic (MHD) wave measurements be carried out by a plasma wave system. The key functional element of the Plasma Wave Sensor is a triaxial search coil with sufficient frequency and dynamic range to detect MHD waves. Three axes are vital to determine the wave modes involved through polarization analysis and determination of the direction of propagation. The search coil system will also detect localized fast- and slow- mode shock waves that will also be Doppler shifted to large frequencies. These objectives require a waveform capture system. To conserve data storage resources, the waveform data could be coupled to a low-data-rate spectrum analyzer for continuous coverage and operate in either a triggered or prescheduled burst mode.

A simple dipole antenna will be able to detect electrostatic emissions up to the plasma frequency (which will reach several megahertz at closest approach) and radio emissions beyond. A single-axis system is sufficient for spectral studies and crude waveform sampling, while a multiaxis system enables polarization and direction-finding analyses, a capability especially interesting for radio burst studies. Again, a low-data-rate spectrum analyzer can be coupled with a high-data-rate, but intermittent, waveform-sampling capability. The length of the antenna elements will be necessarily limited by the available area behind the Sun shield, thus reducing sensitivity. However, anticipated large amplitudes (potentially up to 1 V/m) will limit the need for sensitivity but require a large dynamic range.

2.1.4.1.4 Magnetometer

The Magnetometer and Energetic Particle Composition Spectrometer provide links from the *in situ* measurements along the magnetic field back toward the Sun and the regions sampled by the remote sensing package. The vector magnetometers that have been used in the exploration of the heliosphere and the characterization of planetary magnetic fields (e.g., Mariner 10, Voyager, Pioneer Venus, Mars Global Surveyor, Galileo, Lunar Prospector, etc.) are well suited to measurement requirements of the Solar Probe mission. Total power consumption,

including all analog and digital electronics, and mass for vector magnetometers can be under 1 Watt and 1 kg, respectively. Furthermore, the availability of radiation-hardened, fast, low-power, 16-bit analog-to-digital converters should allow sufficient digital resolution with only 2 or 3 ranges, which simplifies the instrument design. Finally, a triggered burst memory could be contained within the vector magnetometer to allow for added high-resolution data to characterize any dynamic events encountered during Solar Probe's perihelion passage, should there be the possibility of a delayed playback. Coordinated measurements with the fast plasma analyzer and the plasma wave sensor are envisioned to take place at 10^2 Hz in a burst mode.

2.1.4.1.5 Energetic Particle Composition Spectrometer

To study small solar energetic particle events adequately and to distinguish impulsive events, the energetic particle experiment must be able to measure the energy spectra and angular distributions of electrons and ions. The Energetic Particle Composition Spectrometer fills in the suprathermal part of the plasma distribution functions and, combined with Plasma Wave measurements, identifies accelerated particle characteristics as diagnostics for wind dynamics at lower altitudes than those directly sampled by the probe and for plasma turbulence. Identifying the acceleration mechanisms, locating the source regions of energetic particles, and determining the role of plasma turbulence in the production of solar wind and energetic particles is accomplished with the Energetic Particle Composition Spectrometer operating with the Fast Solar Wind Ion Detector and Plasma Wave Sensor. Along the entire trajectory, particles with sufficient gyroradius will be easily detected behind the heat shield.

2.1.4.2 Remote Sensing Experiments

2.1.4.2.1 Introduction

Constructing the three-dimensional density configuration from pole to pole and determining the subsurface flow pattern, the structure of the polar magnetic field, and its relationship with the overlying corona are accomplished with the instruments in the Remote Sensing Package. The strawman remote sensing instruments depend on new techniques developed originally for image stabilization in commercial video cameras, X-ray imaging of laser fusion experiments, and tomographic reconstruction of 3-D structures. Although Solar Probe has unique advantages as an imaging platform, substantial technical challenges to the instrument design are presented by the high thermal loads of the close solar encounter. Other challenges occur because of the limited mass, power, and telemetry of this mission.

The Solar Probe objective is to resolve magnetic structures over the polar cap with a resolution on the order of the mean free path of photons in the photosphere or about 75 km. When the spacecraft is near the equator, the spatial resolution will increase to about 20 km.

2.1.4.2.2 Visible Magnetograph-Helioseismograph

Given the severe spacecraft limitations, the most critical scientific measurements that can be made of the solar disc in the visible are, in order of priority: the magnetic field, a proxy for the magnetic field, and the continuum intensity. Although, it is desirable to measure the full vector field, both measurement complexity and the data rate implications make such measurements extremely difficult. For the solar polar regions, the magnetic field is most likely to be clumped in isolated intergranular regions and oriented nearly vertical to the surface. Thus, Solar Probe instruments will be looking nearly straight down on the fields, so that the longitudinal Zeeman components contain most of the information. To measure the longitudinal component of the magnetic field requires spectral isolation of a portion of a magnetically sensitive line and right- and left-circular polarization analyses. In order to measure the longitudinal Zeeman effect, one wing of a Zeeman-sensitive line must be isolated. This requires a spectral bandpass of 0.1 Å.

As one example of an imager that can measure the Zeeman effect, spectral isolation can be accomplished using a solid Fabry-Perot interferometer (F-P), and polarization separation can be achieved with a polarizing beam splitter and a quarterwave plate.

The orbital trajectory presents two problems for an F-P measurement, motion blur and the Doppler shift. Both are caused by the high speed of the spacecraft along the orbital path. The exposure time for a magnetogram measurement is between 200 and 400 ms. From Table 2, motion blur is only a problem at closest approach. In the polar regions, the spectral shift is most severe. During Solar Probe's inbound phase, the velocity component toward the Sun causes a blue shift of spectral lines. After closest approach, there is a similar motion away from the Sun which causes a red shift.

Consider Fe I 6302 Å ($g=2.5$) as one example for magnetic measurements to illustrate the point. As the spacecraft encounters the Sun, the velocity toward the Sun increases until 90° solar latitude and then decreases to zero at 0° latitude. From Table 2 above, the wavelength shift at 90° is 3.24 Å. When a F-P is tilted, it shifts its transmission peaks toward the blue proportional to the square of the tilt angle. Assuming that the F-P is at the design wavelength of 4389 Å at normal incidence and has a solid spacer with index 1.5, a tilt of 2.3° is required to shift 2.26 Å. (This assumes that magnetograms are only made on the inward portion of the encounter.) If tuning is accomplished mechanically, a range of 3° is probably sufficient to cover both the velocity shift and the temperature shift of the etalon due to changes in the

temperature of the experiment section of the spacecraft. An accuracy of 50 arc-s (216 steps) is sufficient to set the wavelength to 0.05 Å. An electro-optically tuned F-P could also be used.

If a single F-P is used, it probably would have a Free Spectral Range (FSR) of 2 Å (a finesse of 20), which is too narrow to be isolated with an interference filter. However, a pair of solid etalons with thickness ratios of 3 to 4 would have a FSR of 8 Å. All etalons made of the same material have the same wavelength shift with angle. Therefore, the pair of etalons can be bonded together to form a single - Double Etalon Filter (DEF). DEF filters were built during the development phase of the H_α telescopes for Skylab and worked very well. A 0.1 Å DEF could be effectively blocked by an all-deposited 5 Å thin-film interference filter. The blocker has a temperature sensitivity of about 0.2 Å/°C and would not require temperature control, if the temperature of the spacecraft is controlled to +/- 50°C. If the temperature of the spacecraft is not controlled to that level, temperature control or tilt adjustment could be used to compensate.

Determining the proper wavelength setting can be accomplished by scanning the DEF through its full tuning range. This task is somewhat complicated because the spacecraft is moving rapidly across the solar surface. But by adding all the pixels in the image together, it should be possible to make a mean spectral scan sufficient to establish the proper set point for the DEF. This technique has been used on the ground to set the wavelength of tunable filters. It is also used on the MDI experiment of SOHO to set the wavelength of its 0.05-Å filter.

If a direct magnetic measurement is not possible, the next most interesting indicator of the magnetic field locations is provided by images in the CH bandhead, the G-band. The bandhead is sensitive to the local heating in the flux tubes, and, thus, the intensity is a proxy indicator of magnetic field. Unfortunately, when flux tubes exceed 300 km in diameter, the CH bandhead no longer brightens, so that all the magnetic field locations are not indicated by local increases in G-band intensity. However, virtually all small bright points in the G band are coincident with compact magnetic structures. Since the poles are far away from any active regions, it is reasonable to assume that virtually all of the magnetic field is in the form of small flux tubes, and, hence, a G-band image is a good proxy indicator for the locations of magnetic field.

The best ground-based images in the G band show structures of 100 km. The corresponding magnetic features are always larger. There are several reasons for the difference in size, but the largest contribution to the size increase is "seeing blur." For Solar Probe, it would be extremely interesting to know the difference between the sizes of structures seen and at the same time map the magnetic field.

A well-exposed, diffraction-limited G-band image can be made with a 12-Å filter in an exposure time of 10 ms. This means that a simple imaging system using a fast frame-transfer device can make images without use of a shutter and that image motion blur is not a problem.

Using onboard image compression, a data rate of 1 bit per pixel should be achievable. For the minimum image set, ten 256 x 256 images for each wavelength region every 10° of solar latitude, or 6.5 megabits/wavelength for imaging, are desirable. Each statistical distribution of magnetic elements is about 400 bits; sets of 10 every 10° of latitude yield 40 kilobits/wavelength.

2.1.4.2.3 EUV Imager

From Table 2, to achieve 20 km spatial resolution at the solar equator, a 2 arc-sec angular resolution telescope is required. At EUV wavelengths, the optical quality required for diffraction limited imaging cannot be achieved with any known polishing techniques. However, it is possible to polish both EUV and x-rays mirrors to sufficient quality to achieve 2 arc-s resolution. Such mirrors at 4 and 20 R_S can detect 20 and 128 km structures, respectively. If the telescope is diffraction limited, a diameter of 0.314 cm will suffice. Each image will consist of 256 x 256 pixels of 8 bits each.

2.1.4.2.4 All-Sky, 3-D Coronagraph Imager

The more-local environment through which the probe is flying is characterized by an All-sky, 3-D Coronagraph Imager that can identify the larger structures that are being locally sampled by the *in situ* instruments. The all-sky coronagraph imager will image the ambient and surrounding corona in white light.

The All-Sky, 3-D Coronagraph Imager has 1° angular resolution and 0.5% photometric accuracy. The detector dynamic range of >1000 allows imaging of scenes with large brightness variations. Exposures are kept to <1 minute to avoid image blurring due to spacecraft motion.

2.2 Description Of Spacecraft Concept And Mission

The Solar Probe Mission has been designed in response to the science objectives identified by the Solar Probe Science Definition Team. What follows is the description of a "reference mission," giving a snapshot of current thinking at the time this AO was in preparation. Because the Solar Probe Mission (part of the Outer Planets/Solar Probe Project) is still in definition, many important details remain to be worked. In fact, major aspects of the entire mission architecture may be changed and improved as a result of the process in which the

selected science investigation teams will become major participants. Only then will a baseline mission be determined and the design of all its elements be brought to closure and implemented. The information that follows is intended to provide proposers with a point of reference and some insight into results of developments that have taken place to date.

2.2.1 Reference Mission

The reference Solar Probe mission for this AO implements a Jupiter Gravity Assist (JGA) trajectory, which is launched in February 2007 on a Delta III-class launch vehicle augmented by a Star 48V upper stage. The flight duration is approximately 3.7 years to Perihelion 1, and up to 8.1 years to Perihelion 2. Figure 3 illustrates the interplanetary trajectory to Perihelion 1, and Table 4 summarizes the major events of the reference mission.

The reference mission calls for a single spacecraft launch on a Delta III-class/Star 48V launch vehicle. The interplanetary trajectory will take the spacecraft first to Jupiter, for a gravity assist, and then on to the Sun. The gravity assist flyby at Jupiter ($10.5 R_J$, retrograde, southern target) rotates the trajectory to a 90° ecliptic inclination and back toward the Sun for the first of two encounters with perihelia at four solar radii ($4 R_S$).

Recorded *in situ* and remote sensing observations of the corona and the Sun are expected to begin at 10 days before perihelion-1. At approximately 10 days prior to perihelion-1 (0.5 AU), high rate real-time telemetry will begin and continue through P+10days. The telemetry rate will vary between 50-70 kbps depending on the tracking station. The end of the primary observation phase for each of the two perihelia occurs at approximately 10 days past perihelion.

During the first perihelion passage, quadrature geometry is available (see discussion below), and science data will be transmitted in real-time with high-priority data also stored onboard. The stored science data will be played back as soon as possible after the end of the critical data acquisition period (see Figure 4).

2.2.1.1 Baseline Mission

The Solar Probe trajectory uses a northern approach to the Sun reaching a speed in excess of 300 km/s at perihelion. This results in a "pole-to-pole" passage of approximately 13 hours. During this time, the northern and southern high-speed solar wind zones and the equatorial low-speed solar wind zone will be traversed (see Figure 4), along with coronal hole passage(s) and latitudinal coverage of the solar magnetic field. Views of the Sun as seen from the spacecraft at various times during approach for a field of view (FOV) of 30° are illustrated in Figure 5.

In the reference mission design, the time of the first perihelion is selected to allow the quadrature geometry (Sun-spacecraft-Earth angle = 90°), which assures a continuous high-rate data link to Earth through the dual-purpose thermal shield/high-gain antenna of the spacecraft. The Project expects to provide such geometry at the first perihelion but has not yet assessed the feasibility of quadrature for the second perihelion passage. The time of perihelion is also selected such that the position of the Earth allows Earth viewing of the perihelion longitudes just prior to spacecraft overflight.

Because the high-gain antenna is body mounted, a time period will occur during the first encounter such that the direction of the Earth will be outside the pointing capabilities of the high gain antenna while maintaining the necessary shield pointing for thermal control. This time period is expected to occur from perihelion -10 days to perihelion -6 days. During this time, the real-time downlink to the Earth will not be possible, and data storage will be necessary. Real-time data outage will also occur on the outbound leg from +3 days to +10 days, and again, data storage will be necessary.

Quadrature conditions are not enforced for Perihelion -2; therefore, real-time data return is not implemented for the second perihelion passage.

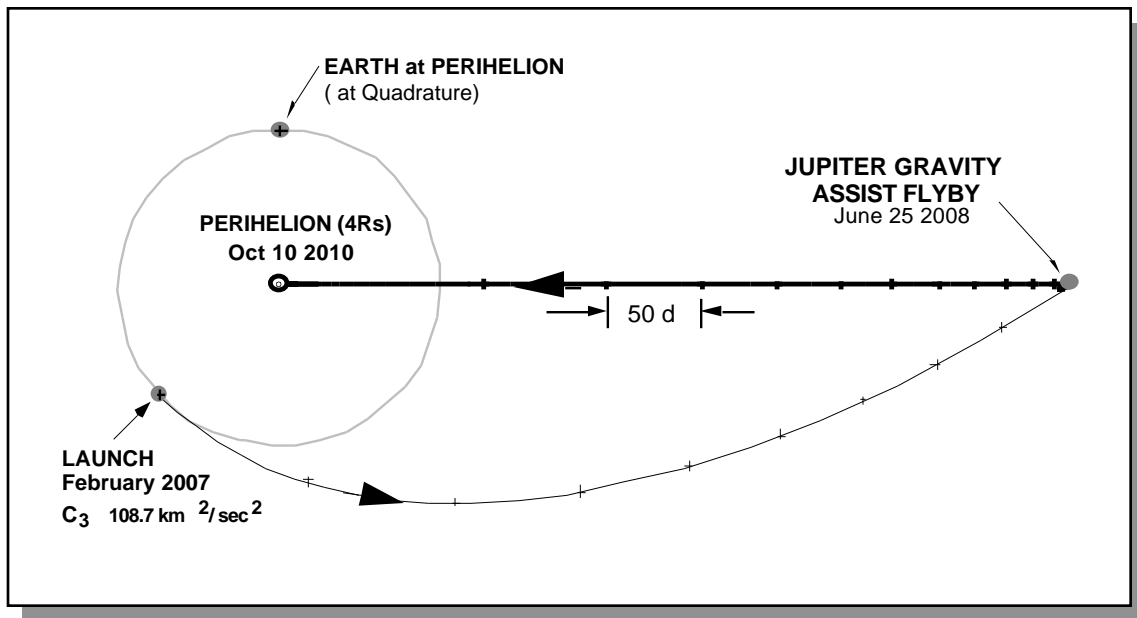


Figure 3. Interplanetary trajectory to Perihelion 1

Table 4. JGA Reference Mission event summary

PHASE	DESCRIPTION	EVENT MARKER
Launch	Launch and Interplanetary Injection	February 15 2007
Cruise 1	Earth to Jupiter Cruise	L+30 d to JGA-15 d
Jupiter Encounter	Jupiter Gravity Assist	June 25 2008
Cruise 2	Jupiter to P1 Cruise	JGA+15d to P1-30d
Encounter Preparation	Navigation and Calibration Phase	P1-30 d to P1-10 d
Start P1 Primary Mission Data Collection	Begin Primary Science Data Acquisition for P1*	P1-10d (0.5 AU)
Critical Science Data Acquisition	Critical Science Data Acquisition for P1	P1±1 d (± 20 R _s) (Perihelion 1 - Oct 10, 2010)
End P1 Primary Mission Data Collection	End Primary Science Data Acquisition for P1	P1+10d (0.5 AU)
Post P1 Transition	Playback and Calibration	P1 + 10 d to P1 + 30 d
Cruise 3	Cruise From P1 to P2	P1+30d to P2-30d
Encounter Preparation	Navigation and Calibration Phase	P2-30 d to P2-10 d
Start P2 Primary Mission	Begin Primary Science Data Acquisition for P2	P2-10 d (0.5 AU)
Critical Science Data Acquisition	Critical Science Data Requisition for P2	P2± 1 d (±20 R _s) (Perihelion 2 - Jan 15,2015)
End P2 Primary Mission Data Collection	End Primary Science Data Acquisition for P2	P2+10 d (0.5 AU)
Post P2 Transition	Playback and Calibration	P2 + 10 d to P2 + 30 d
EOM	End of Mission	P2 + 30 d

* High-rate telemetry not available from P1-10 d to P1-6 d and from P1+3 d to P1+10 d, and from P2 -10 d to P2 +10 d

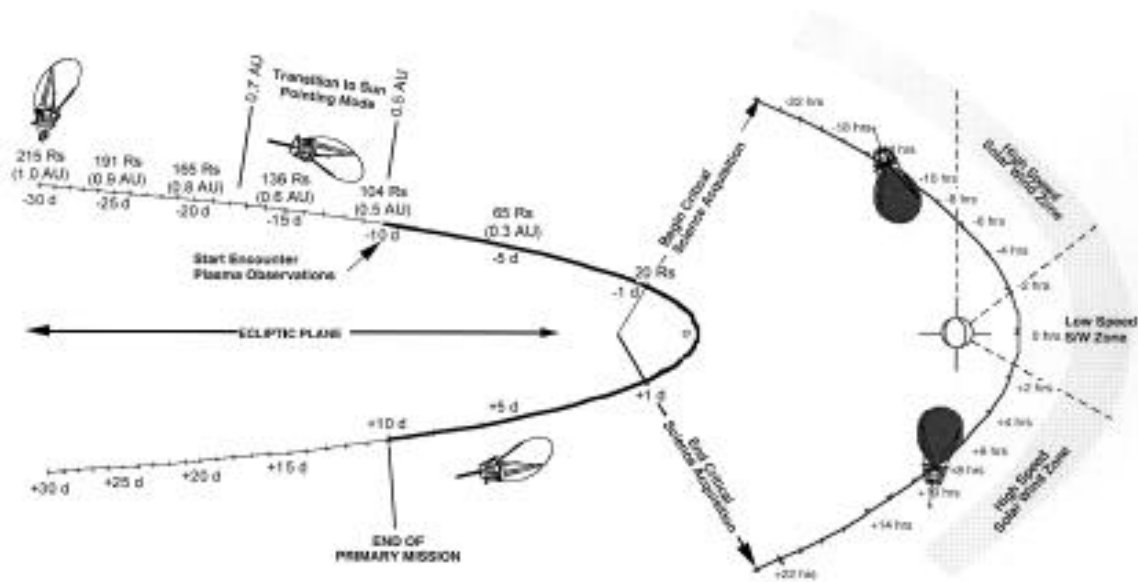


Figure 4. Perihelion 1 trajectory as seen from the Earth

2.2.1.2 Orbit Determination Accuracy

Radiometric tracking alone will be used to deliver the spacecraft to its Jupiter aimpoint to an accuracy sufficient to allow subsequent delivery to the Sun to $4 \pm 0.1 R_S$. Time-of-flight (downtrack) and out of plane components will be controlled only to the extent that a real-time link (quadrature) remains enabled at Perihelion 1. The postmission reconstruction of the trajectory will be to a few km, one sigma, in all three components, for Perihelion 1. If there is no quadrature at Perihelion 2, then the reconstruction will be degraded (to be determined) relative to that at Perihelion 1.

2.2.2 Spacecraft System Design

2.2.2.1 Applicable Standards

The following standards apply:

- The metric system of measurement
- X2000 Mission Data System standards for software implementation
- Reliability, Quality Control, and Safety standards will be tailored to the mission with specific emphasis as appropriate for a long, but cost-capped, mission and in accordance with the project risk management approach

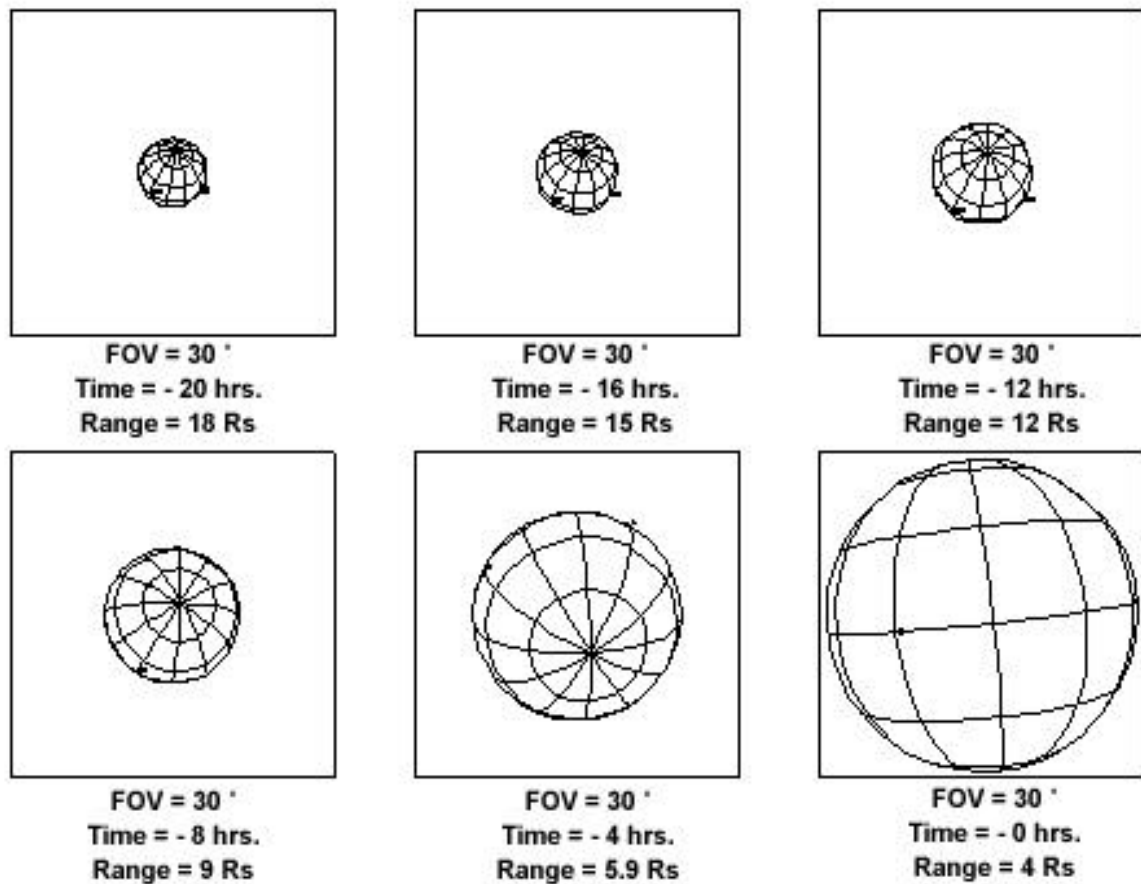


Figure 5. Typical incoming approach perspective

2.2.2.2 System Overview

The flight system for the reference mission is envisioned to consist of a 3-axis stabilized spacecraft bus that houses the engineering and science electronic subsystems, a thermal shield/high-gain antenna subsystem, a propulsion module, and an attached proposed Advanced Radioisotope Power Source (ARPS). The actual spacecraft power source is yet to be defined; however, the ARPS creates the most challenging radiation environment to which the science payload should be designed. Several views of the spacecraft concept are shown in Figure 6. The radiation environment is described in the "Environmental Requirements" document of the Outer Planets Program Library, available over the Internet through URL <http://outerplanets.LaRC.NASA.gov/outerplanets>.

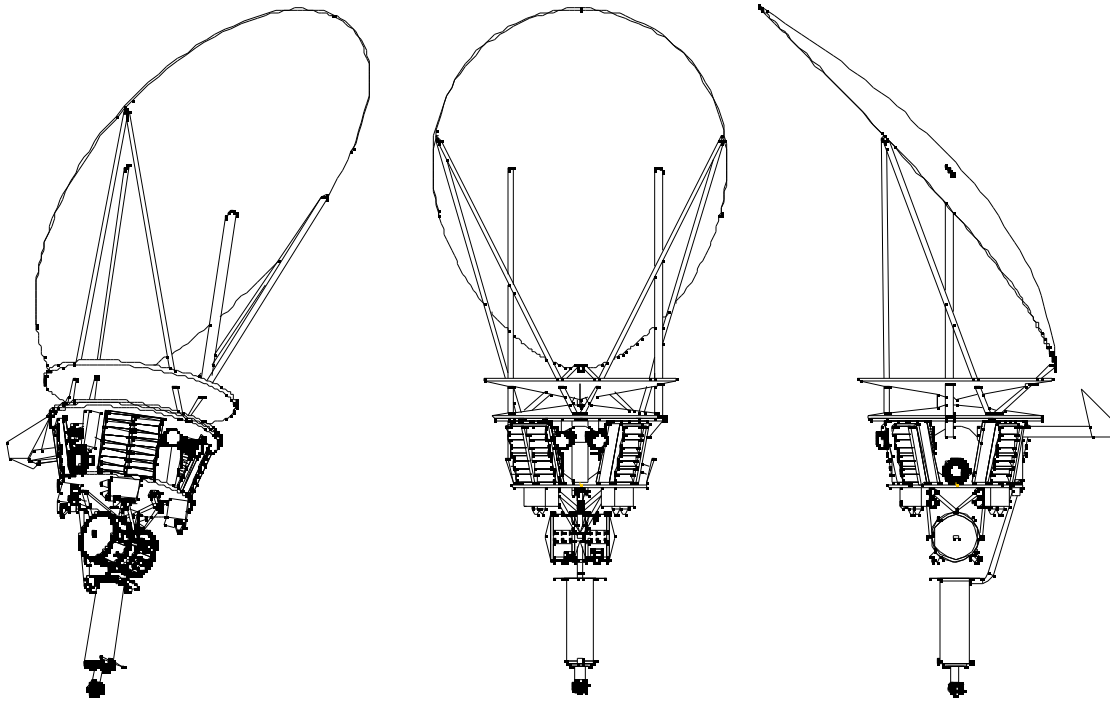


Figure 6. Solar Probe spacecraft

The major hardware elements are depicted in Figure 7.

The current approach assumes that a substantial portion of the engineering avionics subsystems will be designed and qualified through the JPL X2000 development program. The avionics design will incorporate advanced technologies to allow integration of several functions onto a single substrate. By decreasing the size of the electronics while increasing functionality, the avionics mass will be significantly decreased for the Solar Probe mission as compared to missions up to now. The integration of the avionics into a small volume will also reduce the mass of the cabling required to integrate these functions. Additionally, the majority of the electronics developed by X2000 will be radiation hardened to 1 Mrad, and, therefore, very little, if any, additional shielding mass will be required to meet the radiation hardening specification requirement for Solar Probe, which is currently estimated at 35 krad (Si).

Since X2000 is just getting started and has a very aggressive program, some of their deliverable products may not have the performance envisioned today. Whenever possible, this has been foreseen in this AO by the science allocations identified. As X2000 matures and the final flight performance and components are determined, the flight system and instruments will

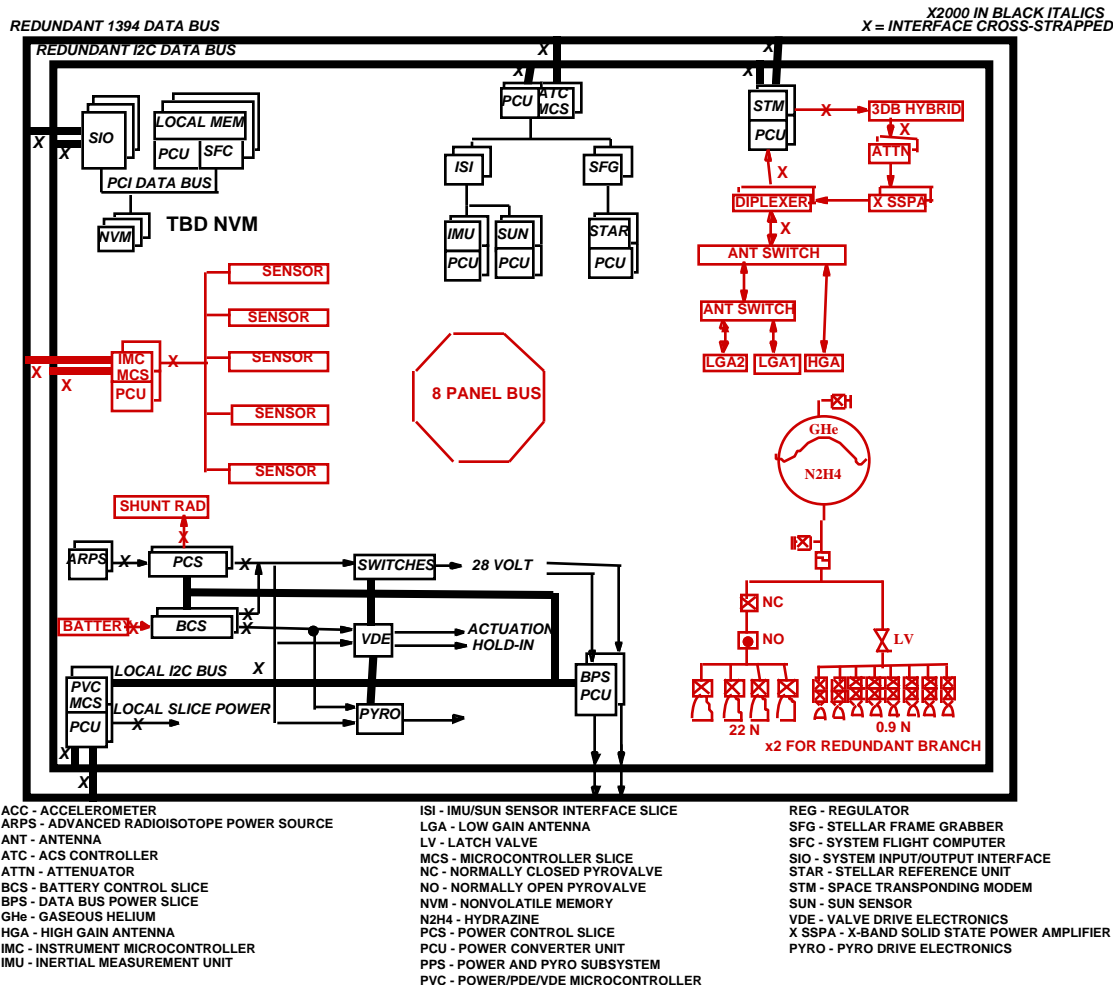


Figure 7. Solar Probe functional block diagram

need to review and finalize the functions and capabilities to be flown. The approach assumed for the integration of the science payload into the engineering system is to minimize the duplication of functions and, thereby, allow maximum science return for the minimum mass, power, and volume. To achieve this, an integrated team will need to determine the distribution of functions between the science payload and the engineering system. Concurrent engineering and teamwork will be required to ensure that the science objectives are met within the resource constraints of the mission.

2.2.2.3 Mass

The allocated mass for the Solar Probe science instruments is given in Table 7 (Section 3.1) including radiation shielding and contingency. The mass allocation places no constraints on where the mass is located within the volume constraints described in 2.2.2.e below. This mass does not include the optical baffles through the HGA/Thermal Shields supporting the nadir viewing optical instruments and the aft instrument boom structure and actuator. Any other booms for instrument mounting must have their mass included as part of the instrument mass.

2.2.2.4 Power

The power allocated for science is given in Table 7 (Section 3.1). This allocation is a maximum for any given point in time during the mission except for possible short-term contamination prevention. The sum of the power for the science complement may exceed this number, as long as operationally the science observations are sequenced so that no more than the allocation is required at any one time. Power transients of up to 100 W for 50 msec are acceptable.

The power subsystem has not yet been determined for this mission. For purposes of a common reference and because the instrument environments would be the most challenging technically, a radioisotope power source is considered here.

The Power Subsystem regulates and converts the output voltage of the ARPS such that loads receive regulated 28 ± 2 VDC. Any high-voltage requirements will be the responsibility of the science investigation. Telemetry will be available on all switched power lines.

2.2.2.5 Volume

The volume accommodations for science instruments are broken into two sets: 1) bus mounted instruments, and 2) instruments mounted on the aft boom. Since all hardware on the Solar Probe Spacecraft must be contained in a small conical umbra and shaded from the intense solar flux, volume is a critical resource for this mission.

The volume allocated to the bus mounted instruments is subdivided into 3 equally sized tapered wedges, as shown in Figure 8. The three 90° wedges are located on the +Y, -X and -Y axes. No margin exists in these volumes; therefore, the instruments must carry volume margin in their instrument proposal such that the defined bus instrument volume will not be exceeded. Instruments may be located on an investigator-supplied boom extending up to one meter from a wedge as shown in Figure 8 (no hardware may extend more than 1.6 m from the spacecraft center line); any shading or thermal control required is the responsibility of the instruments.

Nadir viewing optical instruments are to be located in the +Y and –Y tapered wedges. These two volumes are located where light baffles can be placed in the HGA/Thermal Shield System to allow for direct viewing of the Sun. The light baffles must be greater than a certain length to insure that the heat input to the instruments and bus are acceptable (see Figure 10). Also, the optical baffles must be as far as possible from the high-gain antenna beam. These constraints require that the instrument apertures be as near as possible to the outer edge of these volumes as exemplified in Figure 8.

The volume allocated to the instruments mounted on the aft boom is a cone defined by a combination of the umbra at perihelion and the attitude control angle (see Figure 9). This volume accounts for both the perihelion ($4 R_s$) position and the fully extended position at $8 R_s$. This volume includes the instruments, the boom actuator, and the boom structure.

2.2.2.6 Thermal

All instrument hardware located internally to the bus shall be capable of an allowable flight operating and nonoperating temperature range of -20°C to $+50^{\circ}\text{C}$. The maximum thermal dissipation for each wedge in the bus is 28W. This maximum thermal dissipation includes all solar heat absorbed by the instrument directly or through the light baffles in the HGA or radiated or conducted from any boom extending outside of the main Sun shade umbra in addition to the electrical power thermal dissipation.

For the aft instrument boom, the maximum power dissipation is limited to the maximum heat that the instrument can radiate to space. Estimated minimum boom temperature at Jupiter is $\sim 100\text{ K}$. Minimum survival temperature for boom-mounted instruments at Jupiter must be addressed in the instrument thermal design.

All instruments are responsible for any temperature-control electrical heaters or thermal radiators located on or within the instrument package or specifically required for the conduct of the science experiment. The Project will supply only temperature sensors related to the health of the spacecraft. Any instrument need for additional heat via Radioisotope Heater Units (RHUs) should be specified in the proposal.

In addition to electrical power, the ARPS thermal dissipation could be utilized to heat the bus, if additional heat is required. In addition to the ARPS waste heat, the spacecraft may use Radioisotope Heater Units (RHU's), electrical heaters, the thermal heat shield subsystem, louvers, radiators, and thermal blankets for temperature control.

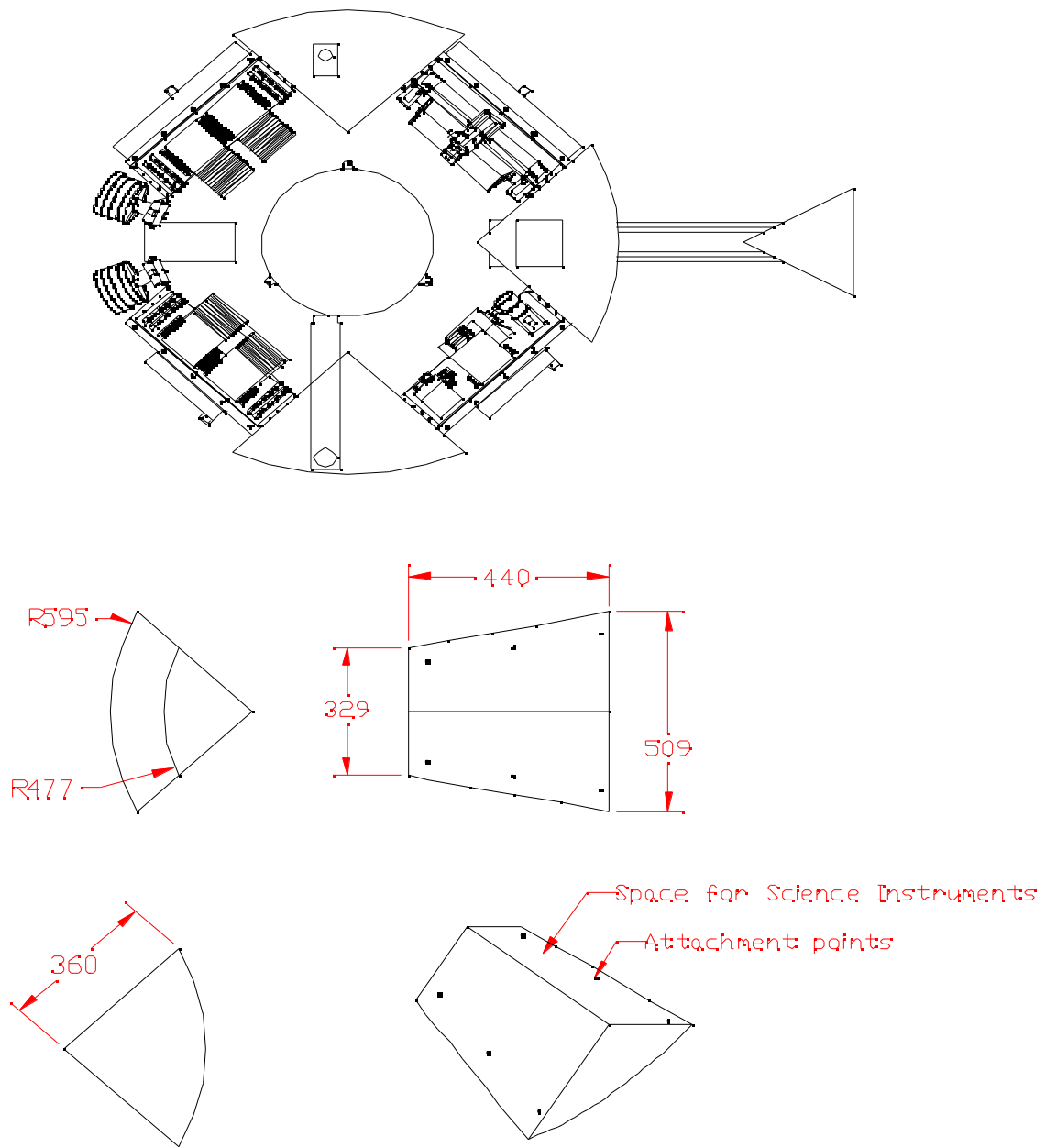


Figure 8. Bus Tapered Wedge Quadrants (dimensions in mm)

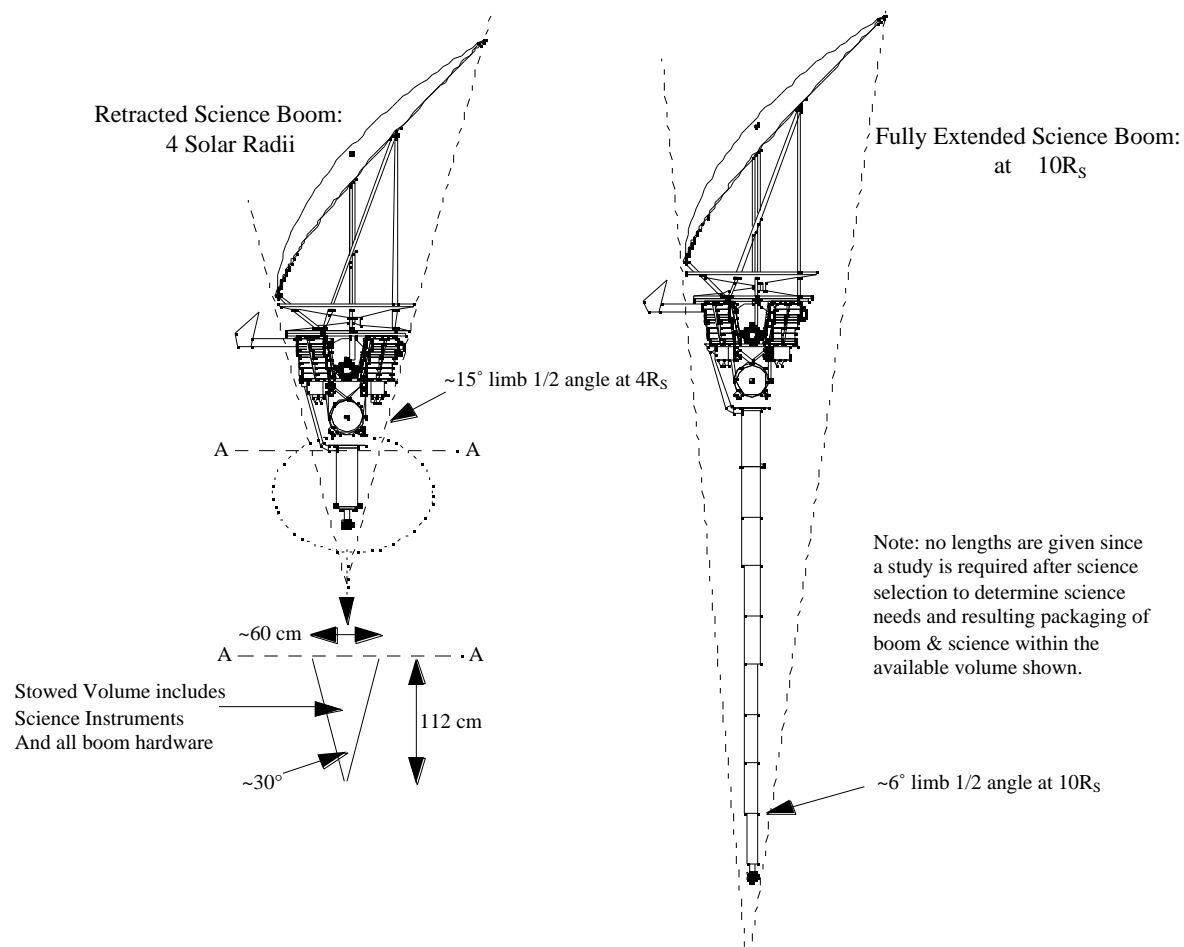


Figure 9. Integrated Science Payload boom volume

The spacecraft thermal design will be capable of maintaining the propulsion subsystem within a 5°C and 50°C temperature range and the bus within a -20°C and 50°C temperature range throughout the mission. The current direct mission has solar distance extremes from 0.02 AU ($4R_S$) to 5 AU.

2.2.2.7 Command, Control, and Data

The spacecraft data subsystem is being developed by the X2000 program and is centered around 2 system flight computers (SFC) sharing engineering tasks and science tasks such as data processing, editing, compression, etc. The SFC will control one redundant high-speed and one redundant low-speed data bus. The protocol standard for the high-speed bus is

IEEE 1394. The protocol standard for the low-speed data bus is I²C. The I²C bus is used for configuration purposes and science instrument commanding.

A generic microcontroller will serve as the standard interface between the data buses and remote terminals such as instruments. Each microcontroller will provide interfaces to the four data buses: prime high-speed, backup high-speed, prime low-speed, backup low-speed. Two microcontrollers each will be supplied by the spacecraft for use by the remote sensing and *in situ* instrument packages (total of four). Their characteristics are defined below and in the "Description Of X2000 Components Available For Use In Instrument Proposals" document of the Outer Planets Program Library, available over the Internet through URL <http://outerplanets.LaRC.NASA.gov/outerplanets>. The mass, power, and cost for these microcontrollers need not be covered within the payload resource allocations of Table 7 in Section 3.1. Any science data processing software that runs on the microcontrollers or the SFC must be supplied and budgeted by the science investigation, however.

The spacecraft data subsystem will include some means of bulk data storage. The current baseline design employs nonvolatile flash memory (NVM).

The planned software operating system for the spacecraft is VxWorks. The planned programming language is C⁺⁺.

The spacecraft will provide time distribution across the command bus with an accuracy of to-be-determined (expected value = 30) msec relative to the spacecraft clock. The instruments can use this to time tag their data when their packets are sent to the spacecraft data system. Otherwise, the spacecraft will time tag the payload packets when received by the data system within to-be-determined (expected value = 30) msec. Each downlink frame is time-tagged to 30 msec relative to spacecraft clock at the time the frame is put together by the data system.

Tentative key requirements for the total data subsystem are:

System processor speed	30 MIPS
High-rate bus bandwidth	100 Mb/s
Low-rate bus bandwidth	100 kb/s
Data storage	less than 6 Gbits

Microcontroller characteristics

speed	10 MIPS
8-bit parallel ports	4
UART ports	2
UART speed	1.5 Mb/s
PCI bus interfaces	1
I ² C subnet	2

Only a fraction of the data subsystem capabilities defined above will be available to support science tasks as reflected in the resource allocations of Table 7 in Section 3.1.

2.2.2.8 Fields of View

The field of view (FOV) for the bus-mounted instruments is 85° half angle on the tapered wedge surface as shown in Figure 10. This FOV surface is good for sensors as well as radiators. In addition, a FOV for a nadir-viewing instrument is shown. A $\pm 20^\circ$ FOV is shown for an instrument of this type that has its own primary thermal shield mounted on a side boom. This FOV could be increased for a longer boom length. For the aft instrument boom, the maximum FOV from the tip of the boom at the fully extended position is 340° . For the fully stowed position, the FOV is 322° (Figure 9).

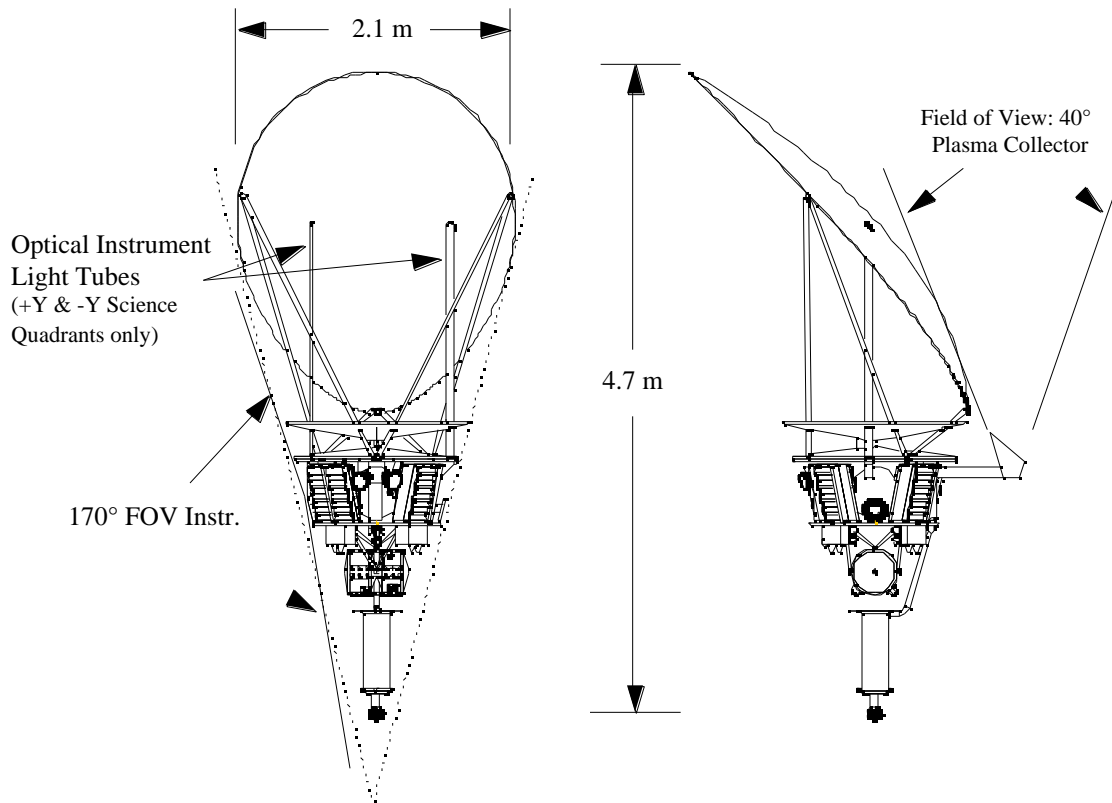


Figure 10. Bus Instrument fields of view

2.2.2.9 Coordinate System and Mechanical Design

The spacecraft coordinate system is as shown in Figure 11. The spacecraft Z axis is located through the centerline of the spacecraft with +Z in the direction the thruster nozzles are pointed (-Z is pointed at the Sun at perihelion). The X-Y plane intersects the Z axis at the base of the bus and is oriented with +X in the direction of the high-gain antenna beam boresight.

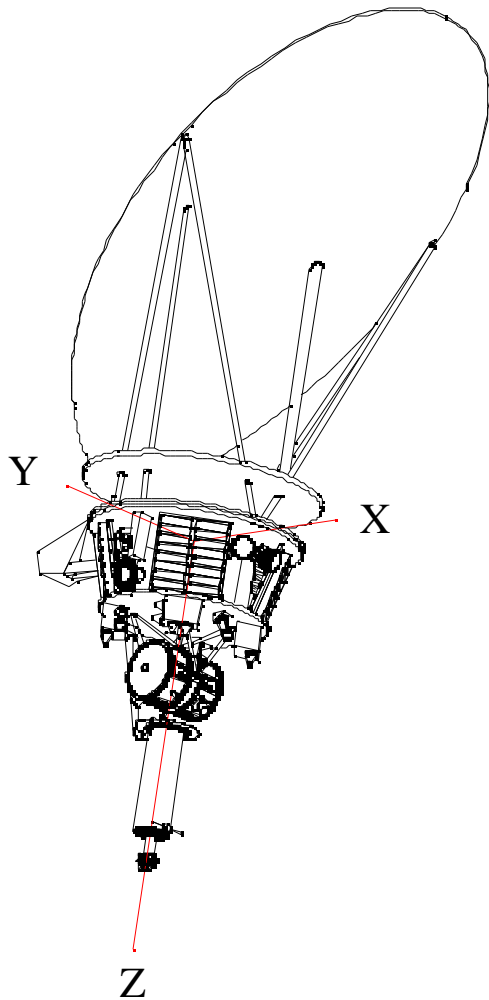


Figure 11. Solar Probe spacecraft coordinate system

The flight system configuration, shown in Figures 2 and 6, consists of the High-Gain Antenna (HGA)/Thermal Shield, the bus, which includes engineering avionics, bus-mounted instruments, the Aft Instrument Boom, the propulsion subsystem, and the power source.

The HGA is used as the primary heat shield. Conical secondary shields are located between the primary shield and the bus. All of the shields are made of various types of Carbon-Carbon. The HGA dish and secondary thermal shields make up the HGA/Thermal Shield subsystem. The unusual dish shape of the off-axis HGA paraboloid is consistent with the quadrature geometry at the first perihelion; quadrature allows for a real-time RF link with Earth at perihelion for the first fly-by. Included in the HGA/Thermal Shield System are two light baffles. The light baffles, made of Carbon-Carbon, allow solar light to be attenuated as it passes through to the instruments that are maintained at room temperature inside the bus.

Below the shield is the "eight" sided bus as shown in Figure 8. Four sides are referred to as bus panels and house the spacecraft avionics. In between the four panels are four tapered wedges. Three of the tapered wedges are for science use as stated in Section 2.2.2.5, and the fourth wedge is used to house the attitude control sensors. The panel material (composite or metal) is to be determined. The four tapered wedge areas will interface with the panels. Instrument interface attachments will be determined after the instruments are chosen. The method of attaching the panels and wedges, along with the bus top and bottom, will require the system to be electrically sealed in order to form a Faraday cage. Loads from the HGA will be transferred through the panels and possibly the wedges depending upon the interface design.

Mounted to the base of the bus is the propulsion subsystem. The current propulsion subsystem is a single-tank, mono-propellant system utilizing hydrazine. The tank will be structurally mounted to the bus close-out plate and located inside the bus structure. The close-out plate will house all of the propulsion components including the four thruster clusters. The close-out plate will also have the integrated science payload boom attachment and the Advanced Radioisotope Power Source (ARPS) attachment bracket.

The aft instrument boom is stowed at launch using a one-time actuator that moves the boom from a launch position to the flight position. The boom extension actuator is located on the boom within the volume described in Section 2.2.2.5. The instruments on the boom are located very close to the ARPS, which produces radiation (gamma and neutron) and a significant magnetic field. These radiation fields are described in the "Environmental Requirements" document of the Outer Planets Program Library, available over the Internet through URL <http://outerplanets.LaRC.NASA.gov/outerplanets>. Spacecraft magnetic fields will be limited as specified in the "Environmental Requirements" document of the Outer

Planets Program Library, available over the Internet through URL <http://outerplanets.LaRC.NASA.gov/outerplanets>. The instruments are also located in an area that will have some minor thruster plume impingement from the Z-axis thrusters. This impingement is not a thermal issue but a contamination issue. The disc shade below the ARPS will help reduce contamination.

Since all cabling to the aft instrument boom must cross the boom actuator, proposals should include a wire count for each instrument on this aft boom. Since larger cables will drive the sizing of the actuator, instruments are encouraged to minimize the wire count over the actuator.

The flight spacecraft will separate from the launch vehicle upper stage adapter at the base close-out plate. The current design uses pyro actuated separation nuts.

2.2.2.10 Attitude Control

The Solar Probe spacecraft will be 3-axis stabilized. Attitude determination will be done using star trackers, gyros, and Sun sensors. Each of these sensors will be block redundant. Gyros will be part of an inertial reference unit. Attitude control and delta-V maneuvers will be accomplished by firing the 0.9-N thrusters of the propulsion subsystem.

Additional functions of the spacecraft attitude control subsystem are to navigate and control the Star 48V injection kick motor. Roll control during injection will be provided by the spacecraft.

Fine pointing will be accomplished using the star tracker for attitude knowledge. Nearly continuous attitude estimation is planned. The star tracker is required to provide 4 steradian attitude determination.

The gyros will be used during maneuvers and for attitude reference during the perihelion passage. The Sun sensor will be used principally for attitude acquisition during cruise and faults. Nadir pointing of the spacecraft -Z axis will be autonomously maintained.

Key baseline requirements for the overall attitude control subsystem are:

pointing accuracy	7 mrad
pointing knowledge	3 mrad
pointing stability	80 μ rad/s

2.2.2.11 Telecommunications

The telecommunications subsystem for Solar Probe reference mission consists of a parabolic high-gain antenna, block redundant 3-watt RF X-band Solid State Power Amplifiers (SSPA's), and block redundant Small Deep Space Transponders (SDST's). A top-level diagram showing the telecom subsystem architecture is shown in Figure 12. The telecommunications configuration shown is a unified uplink/downlink X-band design such that all telecom link functions can be utilized simultaneously.

Command
Telemetry
Doppler Tracking
Ranging

Since both the DSN and flight system have constant power transmitters, the division of power between simultaneous links will vary depending on specific link configurations. This will affect link performance when supporting multiple links at once. Key communications parameters for the Solar Probe mission at perihelion are listed in Table 5.

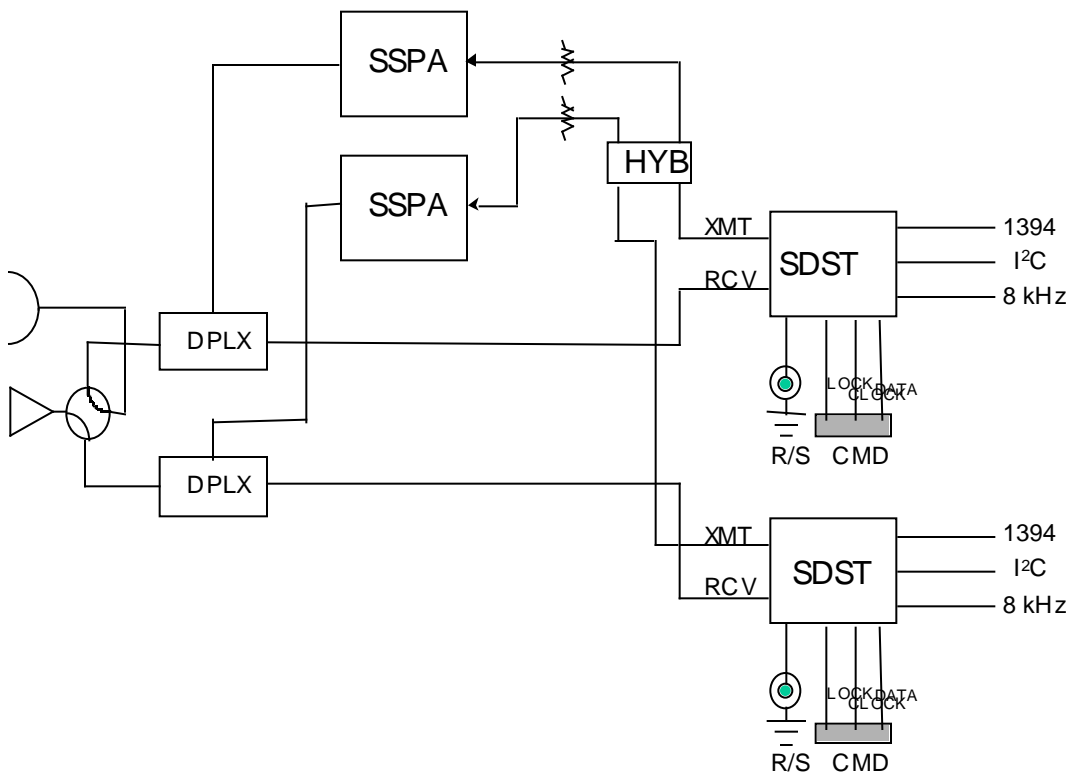


Figure 12. Telecomm subsystem architecture

Table 5. Solar Probe telecommunications parameters at perihelion

<i>Parameter</i>	<i>Solar Probe</i>	<i>Units</i>
Transmitter Power	3	Watts
High Gain Antenna	40	dBi-RCP
Low Gain Antenna	6	dBi-RCP
Science Uplink Command Rate	2	bps
Typical DSN Lockup Time	5	min
Downlink rate (maximum)	88	kbps

Downlink rate is at perihelion assumes 70-m DSN antenna at 20° elevation angle and 90% weather. Uplink command rate assumes 70-m DSN transmitting at 20 kW to the HGA and represents the effective transmission rate for science commands (the actual bit rate sent to the spacecraft is substantially higher).

A representative real time telemetry rate near perihelion is shown in Figure 13. These data are consistent with the assumptions shown in the figure. An additional fundamental assumption is that the amplitude scintillation's caused by coronal perturbations on the downlink are infrequent transient events and will not affect this average telemetry rate performance.

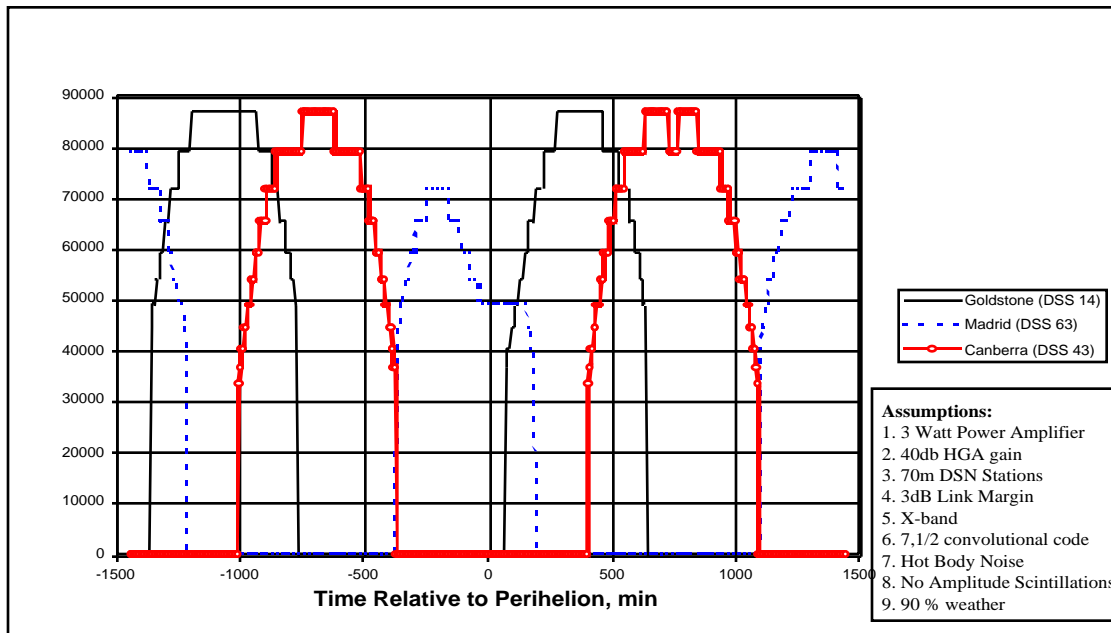


Figure 13. Solar Probe telemetry rate near perihelion for quadrature geometry

2.2.2.12 Propulsion

The propulsion subsystem will provide the required onboard incremental changes in velocity and reaction attitude control capability for the spacecraft over the lifetime of the mission. The total propulsion delta-V is baselined at 90 m/s. This is sized for the Jupiter gravity assist trajectory reference mission with two 4-solar-radii flybys of the Sun. A mono-propellant hydrazine system is utilized. 0.9 N thrusters are utilized for both propulsion and attitude control.

2.2.3 Launch Vehicle

2.2.3.1 Launch Site

The expected launch site will be either the NASA Kennedy Space Center or the U.S. Air Force Cape Canaveral Station, Florida, USA.

2.2.3.2 Launch Vehicle

The final launch vehicle selection has not yet been made. The reference mission assumes that the baseline launch vehicle is a Delta III-class with a Star 48V upper stage.

2.2.4 In-Flight And Near-Sun Environmental Hazards

Generally recognized environmental hazards for Solar Probe fall into three categories:

1. Radiation environment;
2. Dust impacts; and
3. Sublimation from the carbon-carbon thermal shield/antenna.

Hazards (1) and (2) are functions of the ambient (natural) environment; hazard (3) is self-induced by the spacecraft's presence. The level of all three hazards as well as necessary mitigation levels and procedures have been the subject of ongoing debate since the Solar Probe mission was first proposed in the late 1970's. The earliest work was done in conjunction with the incarnation of Solar Probe as the Starprobe mission in the early years (Neugebauer et al., 1978, on the topic of radiation; Goldstein et al., 1980, on the topics of outgassing and spacecraft potential); the most recent comprehensive work was completed at the Solar Probe Environment Workshop [Proceedings of the First U.S.-Russian Scientific Workshop, ed. O. Vaisberg and B. Tsurutani, 1995] held in Moscow, Russia.

These three environmental hazards may further be grouped in order of increasing problem levels:

1. Measurement Contamination - including obscuration of optics and detection of spacecraft-generated signatures in the *in situ* measurements,
2. Measurement Obscuration - measurements dominated by the hazard environment, including both spacecraft-generated signatures and processing and detection failures in electronics caused by an increased radiation background,
3. Instrument Failure - e.g. arcing, structural damage from grain impacts, permanent electronics failure from radiation damage,
4. Spacecraft Failure - Structural failure and/or avionics failure producing the loss of the spacecraft and the mission.

The maximum acceptable hazard level is just prior to encountering level (2), i.e., contamination of measurements is taken as acceptable - but this implies that the contamination can be recognized and worked around or calibrated out.

Other environmental requirements are defined in the "Environmental Requirements" document of the Outer Planets Program Library, available over the Internet through URL <http://outerplanets.LaRC.NASA.gov/outerplanets>.

2.2.4.1 Dust Hazards

There are no data on the magnitude of the dust environment near to the Sun. Observations of scattered light (the F-corona) suggest the presence of dust near the Sun but yield no information on the size distribution, and there is ambiguity in separating thermal from scattering effects in the measured light intensities (Mann and MacQueen, 1995). Within 0.3 AU of the Sun, heating and sublimation of dust is expected to lead to a depletion in the dust environment (dust originates from a variety of sources and is decelerated on Keplerian orbits by the Poynting-Robertson effect) (Mann, 1995). Observations of zodiacal light from the Helios spacecraft suggest that a conservative extrapolation can be made using $r^{-1.3}$ with most of the dust concentrated toward the plane of the ecliptic with an exponential scale-height distribution (Tsurutani and Randolph, 1990; Skalsky and Andreev, 1995). Extrapolations based upon this model suggest a worst case mass flux in ~micron size particles of $10^{-9} \text{ g m}^{-2} \text{ s}^{-1}$ at $4 R_S$. A random hit at typical expected speeds of $\sim 200 \text{ km s}^{-1}$ could, of course, cause structural failure of the spacecraft.

Figure 14 shows the current best estimate of the integral dust particle fluence on the Solar Probe spacecraft over the entire mission.

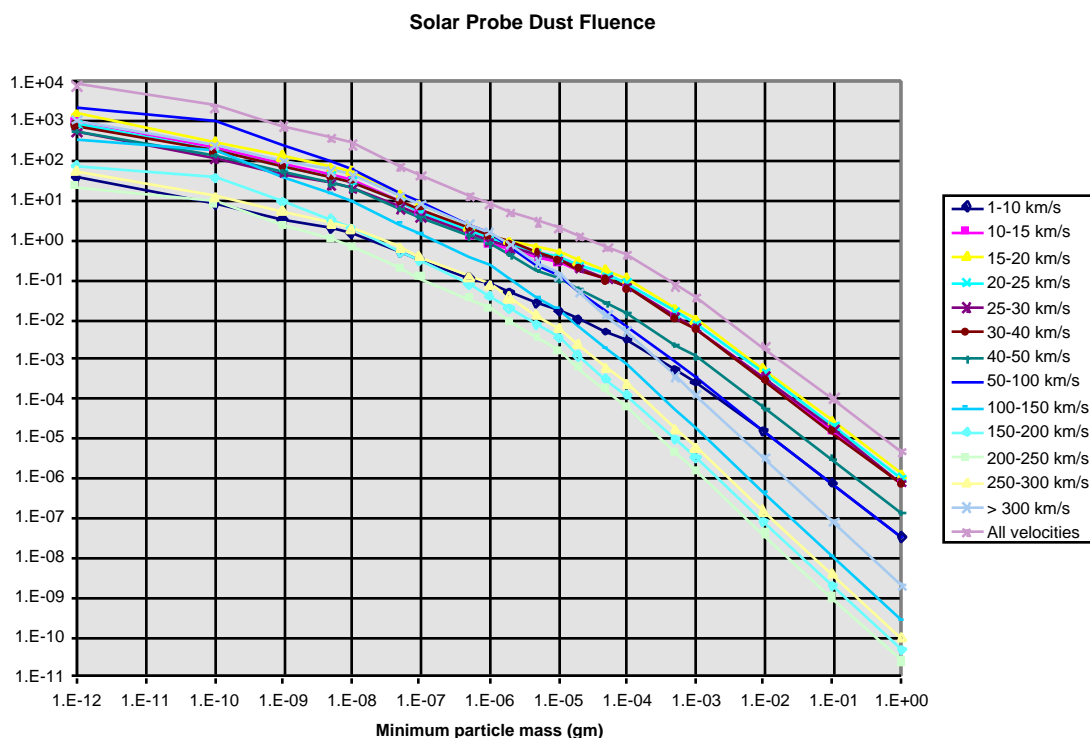


Figure 14. Integral Solar Probe dust particle fluence

Table 6 gives the current best estimate of the expected fluence of particles with masses and velocities great enough to penetrate 100 mils of aluminum assuming a particle density of 2.5 gm/cm³. Fluences are shown for surfaces having random orientation in space, oriented normal to the spacecraft velocity vector (+v), and oriented normal to the spacecraft negative velocity vector (-v). The great majority of the potentially damaging particle impacts will occur during the perihelion passages (inside 0.36 AU) on surfaces facing the spacecraft velocity direction, which will be on a side of the spacecraft parallel with its Z axis. Instruments will need to provide their own protection against such micro-meteoroid impacts.

Table 6. Fluence (number/m²) of 2.5-gm/cm³ particles on the Solar Probe spacecraft that will penetrate 100 mils of aluminum

Time period	Surface orientation		
	random	+v	-v
Through first perihelion	22.8	75.4	0.0023
Through second perihelion	46.4	153.4	0.0071

2.2.4.2 Radiation Hazard

The Solar Probe mission is subject to two different radiation hazards: the magnetospheric environment of Jupiter and the solar coronal environment itself. A Jupiter flyby is required for any Solar Probe mission using near-term propulsion technology due to the requirement for eliminating the angular momentum of the probe acquired by the launch from Earth in order to approach closely to the Sun; the secondary need for a Jupiter flyby is the rotation of the heliocentric probe orbital plane to $\sim 90^\circ$ to the plane of the ecliptic. Launch dates over the next two decades require a Jupiter flyby to within 10 Jovian radii (and as close as $\sim 5 R_J$). This region has been well-explored by the Pioneer 10 and 11, Voyager 1 and 2, Galileo, and Ulysses spacecraft.

For a $\sim 10 R_J$ flyby distance, the expected radiation environment is ~ 35 krad with 100 mil of Al shielding. By using approved parts lists and introducing functional redundancy of appropriate subsystems, this level of radiation background is easily dealt with. Similar remarks apply to single event effects produced by galactic cosmic rays and/or solar proton events (Garrett, 1995).

The radiation hazard provided by the Sun itself remains unknown. Both shock acceleration and direct (flare) acceleration have been implicated in producing particles seen in the 10-100 MeV energy range. Work by Tsurutani and Lin (1985) and Reames (1995) have indicated that the dominant component of the proton flux at 1 AU is due to shock acceleration. Such shocks occur ahead of fast Coronal Mass Ejections (CME's), which occur primarily during solar maximum. Ulysses has indicated that CME-driven shocks can exist at high heliolatitudes (Gosling et al. 1997) with significant particle acceleration occurring.

Wu et al. (1995) have indicated that CME-related shocks first form at a substantial distance from the Sun (typically $15-20 R_S$). Additionally, since high Mach number shocks are more effective at accelerating energetic particles, the near-solar particle fluences would be less than an inward scaling of r^{-2} (fluence) or r^{-3} flux (Feynman et al., 1995).

Solar Probe will be approaching the Sun from high latitudes and will pass over the near-equatorial active regions relatively quickly at perihelion. Both parts of this trajectory are good for minimizing the particle flux/fluence. Kiplinger and Tsurutani (1995) have examined the probability of a flare occurring when Solar Probe is within $\pm 30^\circ$ of the solar equator. Using the statistics of Reames [1995], they find the probability to be about 2% during solar maximum.

Clearly, the solar flare fluence/flux at high latitudes also needs to be studied more closely to better understand the quantitative doses.

2.2.4.3 Outgassing-Sublimation Hazard

Outgassing and sublimation can pose hazards to the Solar Probe in several ways. The most important likely problem is that neutrals released from the high-temperature heat shield will become ionized close enough to the spacecraft to either alter the properties of the solar wind ions and electrons or to generate plasma waves that might mask observation of ambient plasma waves. An additional issue is contamination of spacecraft surfaces by deposition of neutral carbon. If the density of the neutral carbon gas is sufficiently low that the flow of carbon neutrals is collisionless, this would not seem to be a major problem because sensitive surfaces could be protected by restricting the line-of-sight to the hot neutral source. Proper prelaunch heat treatment can reduce the risk from outgassing, but as an unavoidable minimum one is left with sublimation. Sublimation rates are discussed in the subsection 2.2.4.4., and in 2.2.4.4.1.; the ion pickup process and estimated mass loss rates are discussed and found to be sufficiently low to prevent interference with the science observations.

2.2.4.4 Sublimation Rates

In the design of the thermal shield, the logic has been the following: (1) sublimation of shield material (carbon) could interfere with measurements of the *in situ* environment (such measurements are the rationale for the mission); (2) shield sublimation is a function of shield temperature; (3) shield temperature must be driven by the "acceptable" outgassing/sublimation/ ablation rate - as determined by another calculation; (4) shield temperature is then determined by the amount of solar loading versus the amount of radiative area. The actual calculations of shield temperature include both radiation and conduction (which is much less important). For the planned Solar Probe heat shield, which also functions as an antenna, there is a hot region near the tip of the shield that dominates sublimation. Measured sublimation rates from graphite have been available for some time [Drowart et al., 1959]. There are preliminary indications (Valentine et al., 1997) that outgassing from various carbon-carbon matrices is about an order of magnitude less, presumably due to surface energy effects.

The tip of the spacecraft heat shield is approximated as having 0.4 m^2 at 2242 K and 0.6 m^2 at 2204 K, which provide the major portion of the strongly temperature dependent sublimation. For SAIC and C CAT carbon-carbon material (low sublimation rate), the loss rates are 0.0046 mg/s m^2 at 2242 K, and 0.0015 mg/s m^2 at 2204 K. Since mass spectrometry data was not available in the Valentine et al. (1997) study, the Joint Army-Navy-NASA-Air Force (JANNAF) thermochemical tables are used to estimate the relative amounts of loss of

various multiatomic carbon neutrals (C_1 , C_2 , C_3 , C_4 , and C_5). The total mass loss rate for the current Solar Probe design is estimated to be about 3.3×10^{-3} mg/s, if the Valentine et al. (1997) study results are used; if the JANNAP tables are used the results would be about 5 times greater (1.6×10^{-2} mg/s). We note that this is the maximum sublimation rate that occurs at $4 R_S$. When the spacecraft is farther from the Sun, the temperature decrease leads to orders of magnitude less sublimation.

2.2.4.4.1 Mass Loss Rate and Interference with Science Objectives

Early on in Solar probe concept studies, it was recognized that the composition of the thermal shield would have a driving effect on how close to the Sun that the Solar Probe could approach before the *in situ* measurements would be corrupted. Goldstein *et al.* [1980] noted that the driving criterion was "...a requirement of no important interference with scientific objectives." In particular, they were concerned that the impact on plasma wave and electron observations be minimal. Positive ions can presumably be separated from *in situ* ions in the plasma measurements on the basis of ionization state and composition. However, sufficiently large mass loss rates could alter the local electric field in the vicinity of the spacecraft adversely impacting plasma and especially electron measurements. Based upon the criterion that the spacecraft float to no more than 20 V with respect to the local plasma (and introducing a safety factor of 5), they derived a maximum acceptable outgassing rate of 3.0 mg s^{-1} . An independent constraint based upon less than a 1% chance of an electron collision with outgassing carbon was an order of magnitude less stringent. Plasma wave and wake effects were not found to be important at this outgassing/ sublimation level. We note that the recent carbon-carbon material test indicates sublimation rates far below this value.

The question of pickup ion effects was investigated by Okada et al. (1995), Goldstein (1995), and Tsurutani et al. (1995). Goldstein looked at the possibility that the pickup plasma would interact with the solar wind plasma via waves that stand in the spacecraft frame. On this basis, the waves of interest are lower hybrid waves and electron cyclotron waves. From the wave impedance for these types of waves, Goldstein (1995) estimated that a mass loss rate of $2.1 \times 10^{-2} \text{ gm/cm}^3$ would result in a maximum potential perturbation in the plasma of about 5 volts, but because of uncertainties in the method of calculation, recommended that the mass loss rate be limited to about $2 \times 10^{-3} \text{ gm/cm}^3$. This work assumed a neutral ionization time of 30 seconds and that the mass was dominated by C_3 ions. Okada et al. (1995) examined the possibility that C_2^+ ions and related electrons might generate plasma instabilities. Using the Kyoto University Electromagnetic Particle Code (KEMPO), they found that there were no substantial waves generated by either the ion or electron pickup. The combined U.S.-Russian panel on Atmospheric and Electromagnetic Environment Group (Tsurutani, et al., 1995) has determined that the carbon/electron pickup process seems to not be a problem for Solar Probe.

The Science Definition Team obtained some simple checks on the above work.

As a check on the ionization rate assumed in the previous studies, W.-H. Ip independently calculated the ionization rates using more recent estimates of photoionization rates and electron impact rates. For photo-ionization and electron impact rates near the Sun he obtained:

Photo-ionization and electron impact rates at 4 solar radii

	Photo-ionization	Electron impact	Total (a)	Total (b)
C ₁	2.4×10^{-2} /s	1.34×10^{-3} /s	2.53×10^{-2} /s	3.07×10^{-2} /s
C ₂	2.6×10^{-3}	2.38×10^{-3} /s	4.98×10^{-3} /s	1.45×10^{-2}
C ₃	2.6×10^{-3}	2.38×10^{-3} /s	4.98×10^{-3} /s	1.45×10^{-2}

Note: The C₁ and C₂ photo-ionization rates are from W. F. Huebner et al., (1992). The solar condition was assumed to be for the quiet Sun at solar minimum. There exist no laboratory data for the photo-ionization cross sections of C₂ and C₃. The electron impact ionization rates for C₁ and C₂ were obtained from D. Shemansky (private. comm., 1997). As with photo-ionization, the electron impact rate of C₃ is assumed to be the same as that of C₂. The electron temperature is assumed to be 10^6 K and case (a) is for electron number density of 10^4 /cm³, and case (b) is for 5×10^4 /cm³.

The effect of mass loading upon directly decelerating the solar wind was found to be negligible. Within about 2 meters of the spacecraft, the pickup ion number densities were found to be comparable to the solar wind proton densities, but this would not affect the observations. (Note this conclusion is based upon the old, higher outgassing estimates based on JANNAF tables rather than the lower estimates obtained in the Valentine (1997) report.). In view of these results, the most likely (if any) source of interference with the measurements would be generation of plasma waves by the pickup ions, thus confusing the interpretation of the waves normally present in the solar wind. It was assumed that the lower hybrid (modified two-stream) instability would be the most likely source of wave growth. This instability typically requires pickup ion density to be about 10% of the ambient ion density (at least, if the instability is to be isolated in the frequency spectrum). For the case of encounter at four solar radii, the maximum growth rate was taken as $0.5 \omega_{LH}$ (ω_{LH} = lower-hybrid frequency), and the minimum growth length was taken as the solar wind velocity divided by this growth rate. On this basis, the minimum growth rate was found to be 120 m , and full growth to saturation is typically found only after $30 / \omega_{LH}$. As the scale size of the ion cloud where the density is 10% or greater is much smaller than 120 m , it is concluded that the lower hybrid instability is not likely to be a cause of interference.

2.3 Mission Development Concept

2.3.1 Flight System Design and Deliveries

Though the three OP/SP spacecraft will be launched over a period of 3-4 years, the initial spacecraft design will be performed by the same personnel assigned to a joint design team. This team will continue into the detailed design of the Europa Orbiter and Pluto-Kuiper Express spacecraft while identifying areas of commonality for incorporation later into the detailed design of the Solar Probe spacecraft. Common subsystem designs will be used wherever possible to minimize the cost of developing and testing each spacecraft.

The OP/SP Project expects to employ the JPL Mission Data System (MDS) as its end-to-end data system. The MDS is currently under development and comprises both flight and ground software used by multimission and project personnel to operate the spacecraft. MDS will be used in software development, system test, and in actual mission operations and will enable the missions to collect, transport, store, and act on both commands and telemetry. The MDS software architecture employs an object-oriented approach. The MDS spacecraft component will provide a standard interface to the science instruments including time synchronization, commands, data acquisition, memory loading, and memory readout functions. The software architecture is designed such that a core set of software functions are coded and used for all missions. Some mission-specific software will be required to specifically address those unique aspects of each mission, spacecraft, and payload. This core architecture will allow for software reuse, reduced cost in the development and testing of the software, smaller flight operations, faster sequence turn-around times, and improved science return in the event of required failure recovery responses.

Science proposers who intend to exploit available spacecraft computer resources will need to be compatible with the MDS software architecture and design, at least for software that is resident in the Spacecraft Flight Computer (SFC). The extent to which any instrument flight software that runs on an internal instrument computer or any investigator-generated ground sequence planning, Ground Support Equipment, or data analysis software will need to adhere to MDS standards will be specified in an OP/SP Software Management Plan. Instrument proposers should plan to have at least one software expert in residence at JPL for at least 6 months prior to instrument PDR for training in the MDS methodology, development environment, and tools. MDS coding will be in C++, and the operating system is VxWorks/Tornado. The required software licenses will be provided by the Project. MDS documentation will be provided including a Development Plan specifying the software development process, coding standards, review criteria, and configuration management approach; a Capabilities Catalog describing the capabilities supported by the MDS

architecture; and a Users Reference Guide. Science instrument providers will be expected to participate in developing command and telemetry dictionaries, associated system design constraints, and instrument flight rules and constraints.

The planned X2000 First Delivery includes multimission avionics, software, and other equipment for the three missions. The recurring cost for the flight equipment is expected to be comparatively low. The propulsion modules and science packages are unique, however, and they will be a significant factor in the total cost of those missions. These mission-unique costs are borne by each individual mission, but by using common flight support and test equipment and common ground and flight software modules, each mission can reduce its integration and test costs.

Whenever possible, leveraging of technology developments supported by other NASA missions and/or technology development programs will be used where the capabilities match the needs of OP/SP. Such arrangements include incorporation of technologies supported by the New Millennium and Mars Programs. Some mission-unique technology (e.g., heat shield/antenna for Solar Probe) requires that OP/SP wholly support the development.

Standard, reasonable services will be provided the instruments during integration and testing at the system integrator's facility and the launch site. These include:

- Sterile dry N₂ purge (to be connected after receipt at the system integrator). It is the Instrument's responsibility to provide this during shipment and delivery into the integrator's facility.
- Office space with telephones and modem connections
- Laboratory space with limited tool capability in the integration facility.

A Spacecraft Test Laboratory will be developed at the system integrator's facility to simulate the spacecraft and software. The instruments shall provide software simulators of sufficient fidelity as well as breadboards and instrument simulators to support this effort.

2.4 Mission Operations Concept

2.4.1 Integrated Mission Flight Operations Team

The Europa Orbiter, Pluto-Kuiper Express, and Solar Probe missions will share a single core flight team and a common mission data system. This approach is enabled by the common X2000 avionics design shared by all three spacecraft together with a large percentage of

common flight software. Each mission will supplement the shared operations capability with a few mission-dedicated personnel including mission planners, instrument representatives, and science investigation teams.

The core flight operations team will be supported by a university-based operations team which will be competitively chosen in 2001. The university team will be delegated selected routine flight operations tasks to enhance the ability to operate multiple spacecraft simultaneously, to support educational outreach, and to provide a potential source of trained new-hires during the 15 years of flight operations. A workstation-based ground data system design makes implementation of a replica Project Operations Center (POC) at a university cost effective. Science workstations that allow science team members to interact with the operations system from remote sites will be developed as part of the ground data system design.

2.4.2 Beacon Mode Cruise

Routine Deep Space Network (DSN) tracking during cruise will be limited to a single, 4-hour pass every two weeks. This limit on telemetry and radiometric data collection and spacecraft commanding during cruise is intended to keep operations team costs low and reflects the new NASA full-cost-accounting policy, whereby missions are charged for DSN tracking time. To prevent a spacecraft anomaly from going undetected by the ground for a period of up to two weeks, a daily spacecraft beacon monitor track will be performed to establish that the spacecraft is on Earth-point and that no onboard event has been detected that requires ground interaction until the next regularly scheduled telemetry pass. The beacon signal generated by the spacecraft is a subcarrier tone that can be received by a small (5 or 10 meter) ground antenna and detected by a low-cost receiver / detector. The daily beacon monitor check for each spacecraft may be a task delegated to the university operations team.

On-board software that supports Beacon Mode operations includes fault detection and containment software that allows the spacecraft to safe itself during cruise for up to 2 weeks without ground action. Advanced engineering data summarization, onboard alarm limit checking, onboard performance trending, and adaptive anomaly data capture capabilities will also be provided.

The assumption is that science instruments are powered off during cruise except as required for instrument survival. Approximately once a year, or as negotiated with the Principal Investigators, the instruments will be turned on, calibrated, and tested, along with encounter sequence macros that have been developed during the year. Extra DSN tracking during this week will be provided to support the additional commanding and telemetry data collection

required. This annual instrument turn-on week will probably be scheduled to occur during planned science team meetings.

OP/SP data management and data transport protocols will be X2000 MDS-based and will exploit multimission TMOD data services that will have been upgraded to support the MDS design. The MDS design assumes a common flight/ground file-based data management framework. Files will be used to package and store logical data units (objects) that may not map well into the packet model. The goal is to have management of both onboard data files and ground data files appear similar to the user. File management will support long-popular storage/access capabilities for numerous types of nontelemetry data products. File-based transport protocols will be provided for both S/C-to-ground and ground-to-ground nodes. Packetization will be provided as the underlying mechanism of flight-to-ground file data transport. The goal is to make packetization invisible to file-based data management and transport. An implication of this approach is that needed time tags and other ancillary data provided in packet headers and ancillary data packets in the traditional packet-based, data-stream-based systems will have to be provided within the data objects/data files.

2.4.3 Encounter Operations

Transition from cruise operations to encounter operations for the Solar Probe mission starts at perihelion - 1 month. Starting at this time, DSN coverage will increase, along with operations team staffing to support higher activity levels and mission critical events. If available within mission constraints, operations resources will be available to support instrument calibration and serendipitous science observations during the Jupiter gravity assist flyby for the Solar Probe mission.

2.5 Project Schedule

The Project Schedule is given in Figure 15.

3. Science Investigations

3.1 Resources for the Science Investigations

Table 7 summarizes the resource allocations for the Solar Probe science payload. The resource allocations are listed in order of criticality. Proposals that fall outside the allocations for the resources of higher criticality will have a lower probability of selection. Proposals that exceed lower criticality resource allocations will not be penalized provided that they also undersubscribe some higher criticality resource.

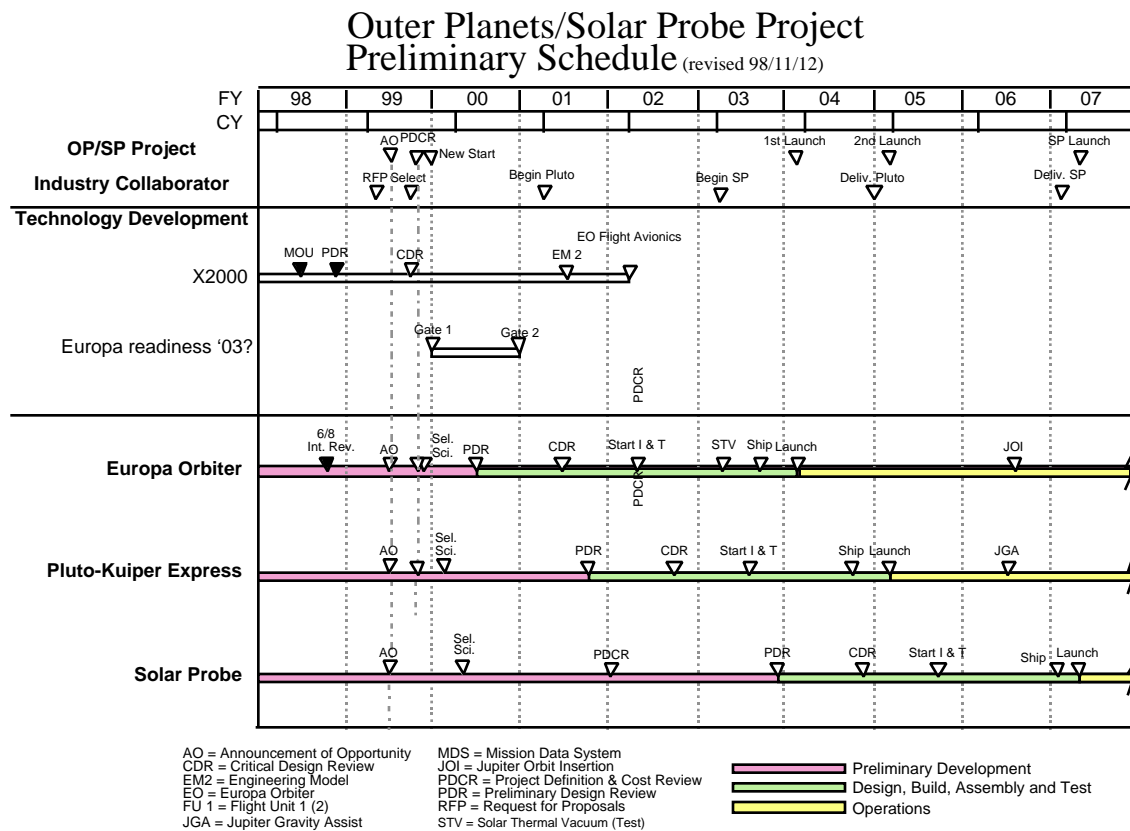


Figure 15. Outer Planets/Solar Probe preliminary schedule

Any instrument covers and mounting booms other than the aft boom structure and actuator must have their mass included as part of the instrument mass. Instruments must also provide their own thermal control system and shades, if located outside the main sunshade umbra. Any instrument purge equipment beyond fittings and internal plumbing that are part of the instrument will not have its mass charged against the above instrument allocations. Any instrument covers must be included in these allocations even if they are jettisoned.

Investigations may exceed the allocated levels of data storage and computer processing MIPS by including the required extra memory or computer as part of their own hardware deliverable. X2000 parts are available for use by science investigators for this purpose, as listed in the "Description Of X2000 Components Available For Use In Instrument Proposals" document of the Outer Planets Program Library, available over the Internet through URL <http://outerplanets.LaRC.NASA.gov/outerplanets>. The cost and mass to cover use of such parts must be included in the instrument totals.

Table 7. Solar Probe science instrument resource allocations in order of criticality

<u>Resource</u>	<u>Criticality</u>	<u>Units</u>	<u>Allocations</u>	
			<u><i>In situ</i> Package</u>	<u>Remote Sensing</u>
Volume	Highest	cm	36x44 wedge w/ 1-m side boom; 36x74 aft cone	2 36x44 wedges
Cost	Higher	M\$ (real yr)	15	16
Power (average)	Higher	watts	10	2.5
Mass	Lower	kg	10	9
Data storage	Lower	Gbits	1.0	1.2
Computer processing	Lower	MIPS	14	16
Data rate	Lower	bps	22	28
Bus bandwidth	Lower	Mbps	12	14
(asynchronous)				
Thermal Power	Lower	watts	28/wedge	28/wedge
Dissipation				

It is anticipated that the teams of *in situ* and remote sensing investigators selected via this AO will be kept small for reasons of efficiency and economy. The total funding available in real year dollars to support these investigator teams (over and above the instrument development costs allocated in Table 7) is as follows:

<u>Team</u>	<u>Development phase</u>	<u>Operations phase</u>
Remote sensing	\$1.8M	\$6.8M
<i>In situ</i> science	\$1.8M	\$6.8M

Table 8 gives the anticipated profile of available funds by fiscal year for each investigation (hardware plus science investigators). Proposals should not plan to exceed these yearly funding levels by more than 20% in any given year unless funding below the indicated level is carried forward from an earlier fiscal year. In no case shall the total funding for the investigation exceed the allocated total.

Table 8. Investigation (instrument and investigators) new obligation authority funding profile guideline in millions of real year dollars for the development and operations phases

Development Phase

	<u>FY00</u>	<u>01</u>	<u>02</u>	<u>03</u>	<u>04</u>	<u>05</u>	<u>06</u>	<u>07</u>	<u>Sum</u>
Remote Sensing	0.5	0.7	0.7	1.1	6.5	7.0	0.9	0.4	17.8
<i>In situ</i> Science	0.5	0.8	0.8	1.2	5.8	6.5	0.8	0.4	16.8

Operations Phase

	<u>FY07</u>	<u>08</u>	<u>09</u>	<u>10</u>	<u>11</u>	<u>12</u>	<u>13</u>	<u>14</u>	<u>15</u>	<u>16</u>	<u>Sum</u>
Remote Sensing Team	0.1	0.1	0.1	1.2	1.6	0.2	0.2	0.9	1.6	0.8	6.8
<i>In situ</i> Science Team	0.1	0.1	0.1	1.2	1.6	0.2	0.2	0.9	1.6	0.8	6.8

3.2 Interaction with the Project

3.2.1 Project Fiscal Policy

The sections below include items that are pertinent for consideration by proposers in preparation of responses to this AO.

3.2.1.1 Budgetary Authority

NASA will annually allocate New Obligation Authority (NOA) to JPL for the Outer Planets/Solar Probe Project based on an Implementation Plan and updates submitted by the Project. In turn, the Project Office will allocate NOA annually to the Project Work Breakdown Structure primary elements based on the NASA NOA, the plans submitted by the leaders of each element (two of whom are the Chief Scientist and the Flight Instrument Development Manager), and the needs of the Project. Each mission (Europa, Pluto, and Solar Probe) has a Project Scientist, and one of them has additional duty as Chief Scientist. The Science Investigation Principal Investigators whom NASA selects through this AO will negotiate their Statements of Work (SOW's), budget submissions, and authority with the Flight Instruments Development Manager, who will be assisted in these negotiations by the appropriate Project Scientist. The resulting SOW and funding schedule will be documented in a contract between JPL and the PI's institution; this contract will be modified, if necessary, through the course of mission development and operations, covering the period of time from contract award to final delivery of science products after the end of the mission.

3.2.1.2 Cost-Capped Mission Budget Environment

Proposers must understand that NASA and JPL budgets for all OP/SP activities are strictly cost-capped. This capped cost includes launch vehicles, integration and interfaces, launch operations, and all flight and ground systems. Mission operations phase costs, including science operations and data analysis, will be similarly capped for each mission. Total project costs will be a primary consideration in all design and development decisions and activities. Other requirements will have flexibility and will be prioritized to provide adequate margins and options for staying within cost and schedule constraints.

3.2.2 Project Organization

Overall project leadership and coordination is provided by the Project Manager and Project Office staff. The project is organized as shown in Figure 16. The Project Scientist is a member of the Project Office staff, is appointed by the Project Manager, and reports to the Project Manager.

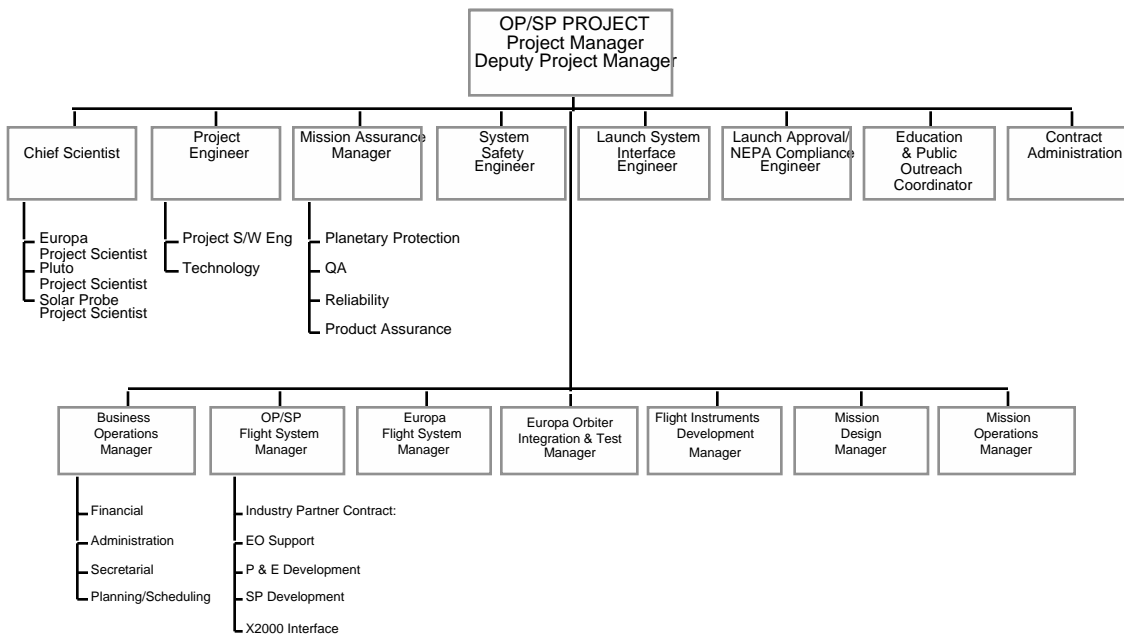


Figure 16. Organization chart for the Outer Planets/Solar Probe Project.

3.2.2.1 Science Investigators as Members of Project Teams

PI's and their lead instrument developers will become members of an integrated implementation team for their respective mission.

Primary interfaces with each mission implementation team will be in the following areas:

1. Trajectory/Navigation/Mission design.
2. Flight System (including mechanical and electronic interfaces, major system trades).
3. Software Development.
4. Mission Assurance (including electronic parts, risk management, quality assurance).
5. Assembly, Test and Launch Operations.
6. Mission Operations and End-to-End Data Flow (including flight/ground Mission Data System).

The avionics, software, and mission data system for the three missions (and other "customer" missions) will be developed in common by the X2000 First Delivery Project, based at JPL, and their numerous partners and contractors in industry, academia, and Government. Some of the electronic parts developed by X2000 will be available for use in science instruments, such as microcontrollers, memory, and power converters (see the "Description Of X2000 Components Available For Use In Instrument Proposals" document of the Outer Planets Program Library, available over the Internet through URL <http://outerplanets.LaRC.NASA.gov/outerplanets>). Each item is intended to be made available commercially and can be considered in the design of the instrument. The OP/SP Project will handle all interfaces with X2000 and will consult with PI teams as appropriate.

3.2.2.2 Relationship Between Science Teams and the Outer Planets/Solar Probe Project

The Mission Scientist for Solar Probe will have overall responsibility for the coordination of the mission's science and the achievement of the mission science objectives through chairmanship of the Mission Science Team, the other members of which will be the Science Investigation Principal Investigators.

Principal Investigators and/or key members of their teams will need to be available for frequent on-line concurrent working sessions. In addition, co-location of key Science Investigation Team members may be required during high-activity periods.

As with the mission design, details of the project organization and interactions will evolve over time to meet the needs of the project and mission.

3.2.3 Encounter Science Team Selection, Participation, and Management

The OP/SP development and operations environment will require that individuals selected to produce the science investigations work closely with JPL and other team members on producing investigation hardware, software, mission design, and the flight system which supports the investigations. It is anticipated that the instrument teams selected in response to this AO will be small and consist mainly of those who will design hardware and software for the mission. Scientists whose role would be primarily in the areas of data reduction and analysis and interpretation of the resulting information will not be funded as part of the initial team in order to save costs.

After launch and as the spacecraft near their science targets, NASA plans to select via a to-be-determined process a broader team of scientists to provide the expertise required to successfully conduct the observations and reduce, analyze and interpret the data. The core of the team, it is anticipated, will be those who designed the investigations during the prelaunch phase, with possible changes reflecting career moves, retirements, and the evolving knowledge base in planetary and solar science. The intent is to retain the crucial expertise needed to fulfill the science investigation, while bringing in new people who can maximize the value of the science returned from the mission.

3.2.4 Mission Assurance Requirements

OP/SP mission assurance requirements for science instruments can be found in the "Instrument Mission Assurance And Safety Requirements" document of the Outer Planets Program Library, available over the Internet through URL <http://outerplanets.LaRC.NASA.gov/outerplanets>.

3.2.5 Principal Investigator Responsibilities

Science instrument Principal Investigators (PI's) are responsible for instrument design and development, fabrication, test, calibration, and delivery of flight hardware, software, and associated support equipment, within project schedule and payload resources. The PI's are responsible for planning and operational support of instrument operation, data analysis, and overall conduct of each of their investigations.

A PI-funded instrument engineer for each instrument will represent the payload at the spacecraft integrator's site as a participant in the integrated development teams and to negotiate interfaces.

The specific responsibilities of the instrument PI include, but are not limited to, the following:

1. Developing an internal management plan and an experiment implementation plan.
2. Ensuring that the design, fabrication, development, and testing of the investigation flight elements are appropriate to the objectives of the investigation and assure qualification to the environmental and interface constraints.
3. Managing hardware and software margin to ensure successful integration and implementation of the experiment.
4. Hardware and software quality assurance and reliability and selection of parts and materials.
5. Ensuring that instrument hardware and software development meets the approved schedules and cost plans.
6. Establishing requirements, Interface Control Documents (ICD's), schedules, and transfer of funds through negotiation with the Project.
7. Ensuring the flight hardware is flight qualified and properly calibrated.
8. Participating in Project Science Group (PSG) meetings and associated working groups. PSG meetings will be held in conjunction with PI Working Group meetings every 6 months.
9. Conducting payload reviews.
10. Participating in Software Working Group (SWG) meetings, as required by the proposed science use of spacecraft computational resources and services to resolve requirements, process issues, and interface issues and to resolve resource allocations and operational timelines.
11. Supporting payload integration and system test procedure development and maintenance and payload hardware and software integration.
12. Participating in flight system tests and integrated end-to-end ground system tests and operation of any payload-unique Ground Support Equipment (GSE) in these tests.
13. Supporting definition of mission database contents, including, but not limited to, flight rules and constraints, sequences, payload telemetry, and commands.
14. Supporting integrated mission data/sequence development and flight software integration.
15. Supporting launch site operations planning, including safety, and launch site system tests at Kennedy Space Center/Cape Canaveral Air Force Station.
16. Planning and executing mission operations.
17. Ensuring that the reduction, analysis, reporting, and archiving of the results of the investigation meet with the highest scientific standards consistent with budgetary and other recognized constraints.
18. Preparing, certifying, and releasing a final data product (to PDS) within six months or less of data receipt on the ground.

3.3 Deliverables

3.3.1 General

The deliveries by the instrument Principal Investigator to the Project include, but are not limited to, the following:

1. Sign a Memorandum of Agreement with the Project that documents resource allocations.
2. Provide and maintain required documentation, including ICD's (see Section 3.5.4)
3. Support development and maintenance of ICD's.
4. Provide monthly Technical Progress Reports and monthly Financial Management Reports.
5. Deliver flight-qualified hardware to the flight system integrator with suitable shipping containers and any protective covers required.
6. Deliver either an Engineering Model, Protoflight unit, or a payload mass simulator and payload data interface simulator to the flight system integrator.
7. Provide necessary payload-unique GSE for stand-alone integration and launch operations.
8. Provide payload unit history log books including power-on time log.
9. Deliver investigation flight software to be resident in the spacecraft flight computer (see Section 3.3.3).
10. Provide timely information to establish and maintain controlled baselines for software interfaces, shared computational resources, mission data, and mission operations timelines and sequences.
11. Archival science data products.

3.3.2 Hardware Delivery

The payload data interface/mass simulator, Engineering Model, or Protoflight unit must be delivered to the flight system integrator's site on or before 16 months before launch. The science payload flight units must be delivered on or before 13 months before launch. Payload flight units must be accompanied by all ground support equipment needed to support system test. Unit history log books shall accompany the flight hardware. Payload flight units must be fully qualified and calibrated before delivery; instruments will not be returned again to the PI.

3.3.3 Software

The OP/SP Software Management Plan will specify requirements on software documentation, testing, source materials, reviews, and metrics.

3.3.3.1 Software Documentation - Software/Computer Systems Interface Control Document (ICD)

Initial definition of operational timeline requirements and related resource demands (characterized by peak and typical parameters) will be negotiated in compliance with resource usage constraints placed on the science payload by the Project and documented in a software-specific section of the Preliminary ICD (with Initial Software Requirements) for:

1. Volatile and nonvolatile memory
2. Process activation frequency and duty cycle
3. Storage demands with storage duration's
4. I/O requirements for all classes (data bus bandwidth, command/telemetry bandwidth) including best available information on compliance with protocol standards or any unique data transfer methods.

Updated information for all items in the Preliminary ICD, with projections of final commitments for all resource demands, plus protocol compliance for all transactions using the spacecraft C&DH, including behavioral characteristics of timing where it is relevant to correct operations of the science payload/mission, is due with the Update Software Requirements ICD.

The committed baseline for all elements of the Software/Computer System Section of the ICD is the third delivery, due with the Final Software Requirements ICD.

3.3.3.2 Software Documentation - Other

Requirements, design, build, test, and evaluation information that provides insight into the software implementation should be provided as they become available, in accordance with the PI's normal development plan.

3.3.3.3 Software Test: Required Evaluation Procedures

Software test procedures are required and are subject to approval. The fidelity of the procedure and level of approval corresponds to the potential risks involved in the procedure. Generally, as the software testing is done in primarily a simulation and Engineering

Development Unit (EDU) environment, the risk is minimal, requiring approval from only the cognizant personnel for the item under evaluation and Spacecraft Test Laboratory (STL) operations. Circumstances that may require further approvals include:

1. Use of flight hardware in the configuration;
2. Requirements for special interfaces, either hardware or software, that may require test setup and verification; and
3. Exclusive operations or continuous operations that produce resource conflicts not reconcilable among other parties.

3.3.3.4 Software Source Materials

The mission load (all executable spacecraft and payload flight software and data) is generated as an integrated load image, including initial/nominal values for all updatable mission data/system files. To develop the mission load, source code for compilation, materials for binding, and data/file load shall be provided in a timely fashion to support software development integration in the Spacecraft Test Laboratory, assembly and integration tests during science payload integration, and mission readiness tests at the launch site. The Final Software Baseline Delivery for launch is scheduled at the time of flight hardware delivery, prior to the start of science integration for final build and characterization of the launch configuration load image. Other postlaunch flight software updates are expected.

3.4 Payload Reviews

The payload PI(s) will be expected to attend the spacecraft Preliminary Design Review (PDR) and Critical Design Review (CDR), ground system reviews, and any informal reviews scheduled by integrated development teams with payload participation requiring the PI rather than the instrument engineer.

Each instrument PI will host a Preliminary Interface Requirements and Design Review (PIRDR) for their investigation. The PIRDR is scheduled as early as possible after the completion of the Functional Requirements Document (FRD)/Experiment Implementation Plan (EIP). Topics include: discussion of the EIP, discussion of the FRD, description of interfaces, I/F verification plan, and description of the safety plan.

Likewise, each PI will host a Final Interface Requirements and Design Review (FIRDR). The FIRDR occurs prior to the mission CDR, at the completion of the payload detailed design. Topics include: status of hardware design, fabrication, test, and calibration, software design and test plans, plans for integration, description of support equipment, finalization of interfaces, command and telemetry requirements, and discussion of environmental and system tests.

Prior to delivery of the flight instrument, each instrument PI will hold a Hardware Requirements Certification Review (HRCR) to ensure that the instrument meets all of its requirements and is ready to be shipped for integration on the spacecraft.

3.5 Documentation Requirements

The following is a list and description of the minimum formal documentation that will be required from instrument PI's:

1. Memorandum of Agreement
2. FRD/EIP/Safety (Combined)
3. GDS/MOS Requirements (Preliminary and Final)
4. ICD Major Milestones
 - Preliminary (with Initial Software Requirements)
 - Final (Start Configuration Control)
 - Update Software Requirements
 - Final Software Requirements
5. Instrument Design Description
6. Payload Handling Requirements List
7. Unit History Log Books
8. Acceptance Data Package

3.5.1 Memorandum of Agreement

A Memorandum of Agreement documents the investigation resource allocation (mass, power, volume and fiscal resources) between the project and each investigation PI. This is written immediately after payload selection and signed by the Project Manager, PI, and spacecraft flight system integrator designee for hardware investigations.

3.5.2. Functional Requirements Document (FRD) / Experiment Implementation Plan (EIP) / Safety Plan

Each instrument PI is responsible for writing a combined Functional Requirements Document and Experiment Implementation Plan for their investigation within 3 months of selection. Contents are negotiated with the project manager, but may be assumed to include:

1. Payload functional requirements,
2. Hardware development-and-test plans and schedule, including reliability and quality assurance plans,

3. Software development-and-test plans and schedule,
4. Cost plan for hardware and software development, fabrication, test, and calibration from selection through launch,
5. Margin management plan
6. Post-launch cost plan for instrument operation, data analysis, and data archiving,
7. Requirements for project support,
8. Personnel and hardware safety plans,
9. Contamination control plan
10. Calibration plans,
11. Science management and investigation plan,
12. Payload portion of range safety plan and payload safety at launch site.
13. Fracture control plan (for Space Shuttle launched payloads).

3.5.3. Ground Data System (GDS) / Mission Operations System (MOS) Requirements

Ground Data System / Mission Operations System requirements due dates are listed below. These primarily address instrument operation requirements and flight rules.

	<u>Solar Probe</u>
Preliminary	9/04
Final	9/06

3.5.4 Interface Control Documents (ICD's)

ICD's are negotiated directly with the spacecraft engineering team in an integrated-development-team environment, with Preliminary ICD's required by the spacecraft PDR and final ICD's under configuration control by the spacecraft CDR. ICD's identify all payload interfaces, including, but not limited to, the volume envelope, mounting, center of mass, electrical and mechanical connections, end circuits, pyro devices, features requiring access or clearance, purge requirements, software requirements, testing, facility support, view angles, clearances, etc.

3.5.5 Instrument Design Description Document (IDDD)

The final design of the payload is documented in an IDDD. The IDDD is due at the HRCR. Included in the IDDD are the parts and materials list.

3.5.6 Payload Handling Requirements

A payload handling requirements list must be supplied prior to the delivery of flight units to the spacecraft integrator. This checklist describes any special handling necessary to ensure the safety of the flight hardware.

3.5.7 Unit History Log Book

The Unit History Log Book accompanies the delivery of the flight hardware.

3.5.8 Acceptance Data Package

The Acceptance Data Package includes (but is not limited to) final drawings, documents, mass properties, qualification data, footprint drawings, final power, etc.

4. Discussion of Nadir Viewing Options

The prime objective of the *in situ* measurements is to find characteristic features in the ion and electron distribution functions near the Sun that provide information on how the solar wind is accelerated. Besides the bulk flow transition from sub- to supersonic acceleration, processes may include wave-particle interactions. Therefore, the plasma detector and the spacecraft must be designed to reveal such processes in the velocity distributions. However, to contain costs it must not be over-designed to obtain more information than is necessary or to look for the solar wind in unlikely directions. Wave damping and other possible acceleration mechanisms will leave characteristic traces in the plasma distribution functions, such as supra-thermal particles, ion jets, etc. Current knowledge of the solar wind indicates that these traces are found in different parallel and perpendicular temperatures, in relative velocities between hydrogen and electrons or hydrogen and other heavier ions, double streams in distributions of individual species, and nonthermal tails or heat flux as a function of the distance from the Sun. For state-of-the-art plasma instrumentation, these requirements pose no problem. However, the challenge lies in the fact that part of the key viewing range, i.e. towards the Sun, is blocked by the heat shield of the spacecraft.

The "aberration" method of viewing the solar wind has been the default option for the Solar Probe. It relies on the aberration of the plasma particles' arrival direction as seen from the rather fast-moving spacecraft (310 km/sec at perihelion) and tilting the spacecraft (when away from perihelion) so that the plasma viewing is close to the edge of the umbra. The solar wind would then be viewed around the edge of the heat shield. Ions and electrons arriving from directions within 15 degrees (or more, because the instrument is not exactly at the apex of the umbra) of the spacecraft axis (nadir) would be out of view. Whether this is a serious loss or not depends on the magnitude and direction of the bulk speed of the solar wind and the

location of the diagnostic features in velocity space with respect to the bulk velocity. The aberration method will work, if the bulk speed of the solar wind is less than twice the spacecraft velocity component perpendicular to the spacecraft-Sun line. However, evidence from IPS, SPARTAN and SOHO measurements cited in Section C.1.c of the "State of Knowledge of the Sun--Taken from the Solar Probe Science Definition Team Report" document of the Outer Planets Program Library, available over the Internet through URL <http://outerplanets.LaRC.NASA.gov/outerplanets> indicates that the speed of the fast solar wind between 4 and 20 R_s is 500 to 800 km/sec. Furthermore, the expected meridional flow of the solar wind at mid-latitudes along the trajectory and deflection by MHD waves will exacerbate this problem at times. The solar wind He and O ions may even be faster than the protons, if He preferentially absorbs wave energy at the He cyclotron frequency. These features would be very important diagnostics of the heating mechanism.

4.1 Solar Wind Plasma Viewing Options

To improve nadir viewing on the Solar Probe with angular and energy coverage as complete as possible, several different approaches should be considered. In principle, those are:

- Minimizing the blocked angular range dynamically by mounting the plasma spectrometer on an extendible boom that keeps the sensor at the anti-sunward tip of the umbra. This minimizes the size of the obstruction, but the nadir direction (± 8 degrees at 10 R_s) is still blocked.
- Viewing of selected pieces of the distribution function through collimator tubes protruding through the heat shield. This provides a few disconnected pieces of the distribution in nadir direction, but keeps the maximum obstruction for contiguous observations.
- Providing true nadir viewing by means of an electrostatic mirror that deflects ions around the heat shield. This allows an almost full field of view, but may be limited to less than 12-18 keV/Q.

To provide better understanding of this problem, we will demonstrate how typical ion distribution functions in the solar wind are viewed by a plasma instrument in these options. Ultimately the choice will be determined by the optimum compromise between the achievable viewing and the impact on spacecraft complexity and resources.

4.2 Plasma Visualization Model

For illustration purposes, a simplified model of the solar wind with a Maxwellian distribution and a temperature anisotropy in T_{\perp} and $T_{||}$ has been chosen. The expected bulk speeds and

temperatures as a function of distance are taken from a model by Habbal et al. (1995). Figure 1.A shows a sample solar wind distribution in color representation for the inbound leg of the trajectory over the pole at $10 R_s$. Shown are a cut in the plane of the spacecraft trajectory ($v_x - v_y$) and a cut in a perpendicular plane ($v_z - v_y$) at $v_x = 890$ km/s. The distribution is shown in the spacecraft frame, i.e., as seen by a plasma instrument. The rest frame is indicated by an additional white cross, offset by the negative spacecraft velocity. The lines inserted in both cuts indicate the fractions of the distribution function that are not visible by a plasma sensor with fixed mounting (dashed line) and extendible mounting (full line). The obstructed portion of the distribution can be viewed up to 12-18 keV/Q using an electrostatic mirror as described in Section 1.1 above. This viewing tool can be visited on the WWW under http://satyr.msfc.nasa.gov/Solar_Probe/ to explore other custom examples.

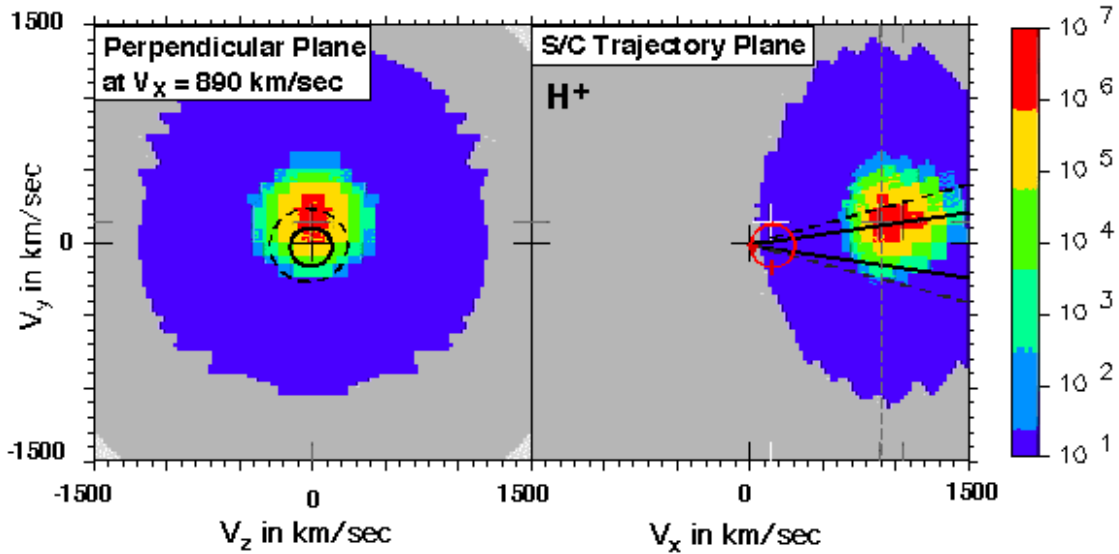


Figure 17. Sample distribution of H^+ with $V_{sw} = 740$ km/sec with $T_{\perp} = 2 \times 10^6$ K, $T_{\perp}/T_{\parallel} = 2$ and a second beam at a differential velocity of +160 km/s, displayed in the spacecraft frame at $10 R_s$. Shown are two cuts: in the plane of the trajectory (right) and in a perpendicular plane at $V_x = 890$ km/s (left, gray line in right panel). The obstructions by the heat shield are shown as wedges and circles in both planes, respectively (dashed line: fixed mounting, full line: extendible boom mounting). An electrostatic mirror covers viewing between the dashed lines. The red circle indicates the motion of the origin of the spacecraft rest frame through velocity space along the spacecraft trajectory.

When referred to radial (v_x) and meridional (v_y) solar coordinates in velocity space, the tip of the spacecraft velocity vector executes a counter-clockwise circle of diameter equal to the speed at perihelion along the entire trajectory and so does the 0-marker of the spacecraft frame in the right panel of Figure 17 (indicated by the circle). The speed at perihelion in a quasi-parabolic orbit is $42/\sqrt{r}$ km/sec, where r is the perihelion distance measured in AU. For Solar Probe, the speed at perihelion is 310 km/s (indicated by the white cross). With this circle, we can easily evaluate the aberration of the distribution function of the plasma at any point along the trajectory. The vector sum of the spacecraft aberration velocity and the velocity of the plasma in the solar frame provides the angle and speed in the spacecraft frame at which the plasma is viewed. In particular, it shows at each point along the trajectory what angles with respect to the spacecraft nadir the plasma instrument must view to see particular features of the distribution function and which features may be obstructed by the shield. For example, on the inbound leg the radial velocity adds to the solar wind velocity, i.e., the aberration effect on the viewing is weakened. A variable, but substantial, cone in velocity space remains invisible due to the obstruction by the shield as a function of distance from the Sun. The narrower cone in Figure 17 represents the obstructed view at $10 R_S$ for the variable distance (extendible/retractable) boom.

The typical variation of the half width of the obstructed cone with distance from the Sun for an extendible boom is shown in Figure 18, along with the variation of the aberration angle for a radial solar wind flow of 740 km/s. While the bulk of the distribution will frequently be obstructed for a plasma instrument on a fixed mounting, the viewing of the bulk flow can possibly be preserved with a minimized obstruction using an extendible boom. However, it should be pointed out here that the figure shows a purely radial flow. A tilt of the magnetic field lines into the probe trajectory, which is very likely over the poles according to the model by Gleeson and Axford (1976), tends to move the bulk flow into the obstructed portion. Also magnetohydrodynamic waves may deflect the wind into or out of this direction. In both cases, the bulk flow could be lost and would have to be reconstructed from the peripheral view without nadir viewing. Even if the very center is not cut out, it will be difficult to reconstruct nonthermal features, such as a nonthermal tail or heat flux. Judging the substantial fraction that may be lost in and near the center of the wind distribution from the example in Figure 1.A, this would constitute a major reduction of the capabilities in a key scientific area for the probe for the inbound polar passage.

4.3 Assessment of nadir viewing options

Given these viewing conditions of the solar wind along the Solar Probe trajectory, we now compare the different options to cope with the requirements with regard to their capabilities and their impact on the spacecraft system. Compared are electrostatic deflection of the solar wind around the heat shield, mounting of the sensor on an extendible boom at the edge of the

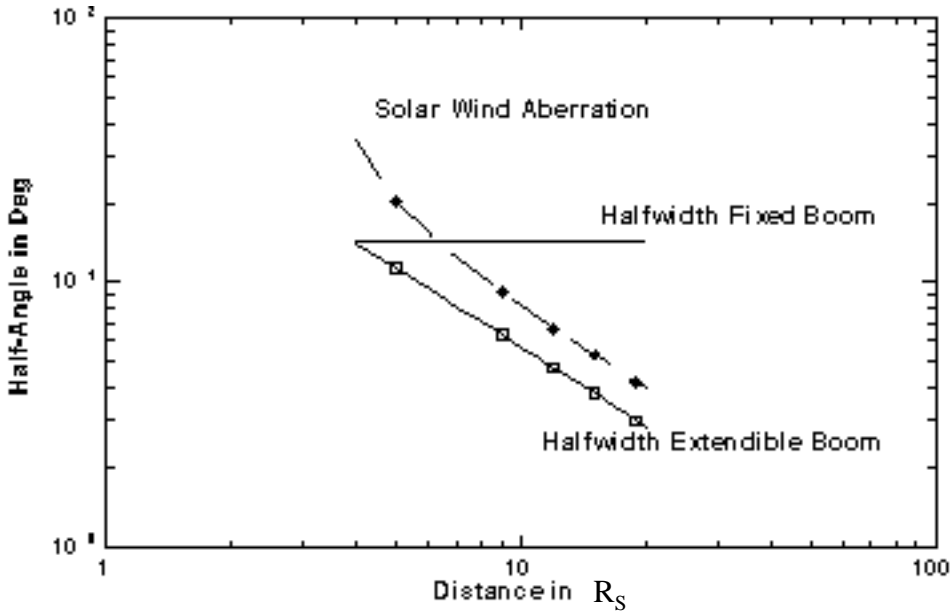


Figure 18. Variation of the half-width of the obstruction cone for an extendible boom, along with the aberration for pure radial solar wind on the inbound trajectory of the Solar Probe. It should be noted that for distances $> 8 R_S$ (over the pole and further outbound) a meridional flow or MHD wave deflection of the solar wind of $\sim 3^\circ$ can move the core of the wind distribution into or out of the obstruction. The halfwidth for fixed mounting is also shown.

umbra, and viewing through apertures in the heat shield with fixed mounting of a sensor at the end of a fixed boom and at the side of the spacecraft bus. A summary of the viewing options, their capabilities and limitations, along with the impact on spacecraft resources and complexity is compiled in Table 1.1.

Only an electrostatic deflection system and/or small apertures through the heat shield (coined "soda straws") will be able to provide true nadir viewing. While small apertures will add a few separated slabs of the velocity distribution at a minimum separation from each other of $\sim 10^\circ$, an electrostatic mirror will be able fill this void for energies up to $\sim 12 - 18 \text{ keV/charge}$ with 5° resolution. Because the "soda straws" require a fixed mounting, contiguous coverage will not be possible in a 30° cone throughout the mission. Even the extendible boom provides more unobstructed field of view. Given the coverage and resolution, electrostatic deflection provides the preferable option to preserve viewing of a substantial portion of the solar wind distribution in particular over the solar poles.

Table 9. Criteria for plasma viewing options

<i>Performance</i>	Electr. Mirror	Extend. Boom	Soda Straws	Fixed Boom	Bus Mount
Viewing	no obstruction $(E/Q)_{\max} = 1.5 \cdot U_m$	minimized central obstruction	several fixed fringes of distribution	large central obstruction (30°)	Partial view at 90° w.r.t Sun
Cleanliness of measurement	local sublimation from instrument shield	None	secondary particles in straws?	None	None
Science Desirability	1	2	3	4	5
<i>System Impact</i>					
Mechanical	launched in position	intermittent motor torque's, stability, one-time deployment after launch	alignment, vibration	None	None
Electrical	HV on boom and mirror, HV/HT cables	intermittent motor magnetic field, retractable cables	None	None	None
Thermal	heat input into bus from shield	negligible	heat input to bus	None	None
Power	HV supply and cables	noncontinuous motor	None	None	None
Mass	mirror, supply, boom, shield	boom, motor	straw structure	boom	None
System Impact	optical alignment on S/C, thermal, cable EMI	attitude control	Calibration on S/C; may change	-	-
Complexity/Risk	high/low	medium/medium	high/low	low/low	low/low

All three improvements over the fixed sensor mounting require additional spacecraft resources and add to the complexity. The "soda straws" present the toughest challenge with their multiple breach of the shield and also with the system requirement for a final sensor calibration performed on the spacecraft. The electrostatic deflection presents a significantly higher challenge than the extendible boom because of its heat impact behind the shield and the high-voltage (HV) and high temperature (HT) integration. However, it provides the preferable science option to preserve viewing of a substantial portion of the solar wind distribution, in particular over the solar poles, which is important to the mission requirements as discussed above.

5. References

1. Feynman, J., B. E. Goldstein, and G. C. Spitale, The radial dependence of solar proton fluences, *Proceedings of the First U.S.-Russian Scientific Workshop on FIRE Environment*, pp. 55-68, IKI, Moscow, 1995.
2. Garrett H.B. et al., Single-event upset effects on the Clementine solid-state data recorder, *Journal of Spacecraft and Rockets*, 32, 1071-1076, 1995.
3. Gleeson, L. J., and W. I. Axford, An analytical model illustrating the effects of rotation on a magnetosphere containing low-energy plasma, *J. Geophys. Res.*, 19, 3403, 1976
4. Goldstein, B., et al., Spacecraft mass loss and electric potential requirements for the starprobe mission, *JPL 715-100*, 1980
5. Goldstein, B., Standing wave effects on electric potential of the outgassing cloud, *Proceedings of the First U.S.-Russian Scientific Workshop on FIRE Environment*, pp. 133-139, IKI, Moscow, 1995
6. Gosling, et al., Ulysses and WIND particle observations of the November 1997 solar events
7. *Geophys. Res. Lett.*, 25, 3469-3472, 1998.
8. Habbal, S. R., R. Esser, M. Guhathakurta, and R. R. Fisher, Flow properties of the solar wind derived from a two-fluid model with constraints from white light and *in situ* interplanetary observations, *Geophys. Res. Lett.*, 22, 1465, 1995.
9. Huebner, W. F., J. J. Keady, and S. P. Lyon, Solar photo rates for planetary atmospheres and atmospheric pollutants, *Astrophys. Space Sci.*, 195, 1-294, 1992.
10. Kiplinger, A. L., and B. T. Tsurutani, Fire under Fire: Proton probabilities at perihelion, *Proceedings of the First U.S.-Russian Scientific Workshop on FIRE Environment*, pp. 273-279, IKI, Moscow, 1995.
11. Lin R.P. et al., Nonrelativistic Solar Electron Events During December 1990 - Results From Ulysses *Geophys. Res. Lett.*, 19, 1283-1286, 1992.
12. Mann, I., Dynamics of dust in the solar environment, *Proceedings of the First U.S.-Russian Scientific Workshop on FIRE Environment*, pp. 154-160, IKI, Moscow, 1995
13. Mann, I., and R. M. MacQueen, Ground-based observations of dust in the solar environment, *Proceedings of the First U.S.-Russian Scientific Workshop on FIRE Environment*, pp. 161-165, IKI, Moscow, 1995
14. NASA Research Announcement 95-15, Advanced Instrument Concepts for a Near-Sun Flyby, 1995

15. Neugebauer, M., L. A. Fisk, R. E. Gold, R. P. Lin, G. Newkirk, J. A. Simpson, and M. A. I. Van Hollebeke, The energetic particle environment of the Solar Probe Mission, *JPL 78-64*, Jet Propulsion Laboratory, Pasadena, CA, 1978.
16. Okada, M., B. T. Tsurutani, B. E. Goldstein, A. L. Brinca, H. Matsumoto, and P. J. Kellogg, Investigation of possible electromagnetic disturbances caused by Spacecraft Plasma Interaction at 4 R_s , *Proceedings of the First U.S.-Russian Scientific Workshop on FIRE Environment*, pp. 108-116, IKI, Moscow, 1995.
17. Reames D.V., Richardson I.G., Wenzel K.P., Energy-Spectra of Ions From Impulsive Solar-Flares, *Astrophys. Journal* 387, 715-725, 1992.
18. Reames, D.V., Focused Interplanetary Transport of Similar-to-1 MeV Solar Energetic Protons Through Self-Generated Alfvén Waves, *Astrophys. Journal* ,424, 1032-1048, 1994.
19. Reames, D.V., Solar Energetic Particles-A Paradigm Shift *Rev. Geophys.*, 33, 585-589, 1995.
20. Skalsky, A. and Andreev, V., The Dust in the Solar System: The Interplanetary Space, The Jovian and Solar Environments, *Proceedings of the First U.S.-Russian Scientific Workshop on FIRE Environment*, pp. 140-153, IKI, Moscow, 1995
21. Temerin, M. et al., Nonlinear Ion Heating in Magnetized Plasma by Monochromatic Low-Frequency Waves, *IEEE Transactions on Plasma Science* 14, 910-914, 1986.
22. Tsurutani, B. T., and Lin, R. P, Acceleration of >47keV Ions and >2keV electrons by interplanetary shocks, *J. Geophys. Res.*, 90, 1, 1985.
23. Tsurutani, B. T., V. N. Oraevsky, H. Matsumoto, S. I. Klimov, et al., Report on Combined Atmospheric and Electromagnetic Environment Group, *Proceedings of the First U.S.-Russian Scientific Workshop on FIRE Environment*, pp. 256-258, IKI, Moscow, 1995
24. Tsurutani, B. T., and J. E. Randolph, Origin and Evolution of Int. Dust, ed. A. Levaxeur-Regourd and H. Hasegawa, Kluwer, 29, 1990
25. Vaisberg, O. and B. T. Tsurutani, eds., *Proceedings of the First U.S.-Russian Scientific Workshop on FIRE Environment*, Space Research Institute, Moscow, Russia, 1995
26. Valentine, P. G., P. W. Trester, and R. O. Harrington, Mass Loss Testing of Carbon-Carbon at High Temperatures, General Atomic Report GA-C22515, 1997
27. Wu, S. T., W. P. Guo, M. Dryer, B. T. Tsurutani, and O. L. Vaisberg, Evolution of Coronal MHD shocks into interplanetary MHD shocks, *Proceedings of the First U.S.-Russian Scientific Workshop on FIRE Environment*, pp. 266-272, IKI, Moscow, 1995